

Adjoint Approaches for Optimal Active Flow Control

Nicolas R. Gauger, Anil Nemili and Emre Özkaya

Computational Mathematics Group, CCES
RWTH Aachen University, Aachen, Germany



Felix Kramer and Angelo Carnarius

Institute of Fluid Dynamics and Technical Acoustics, ISTA
Technical University of Berlin, Berlin, Germany



Frank Thiele

CFD Software Entwicklungs- und Forschungsgesellschaft mbH
Berlin, Germany



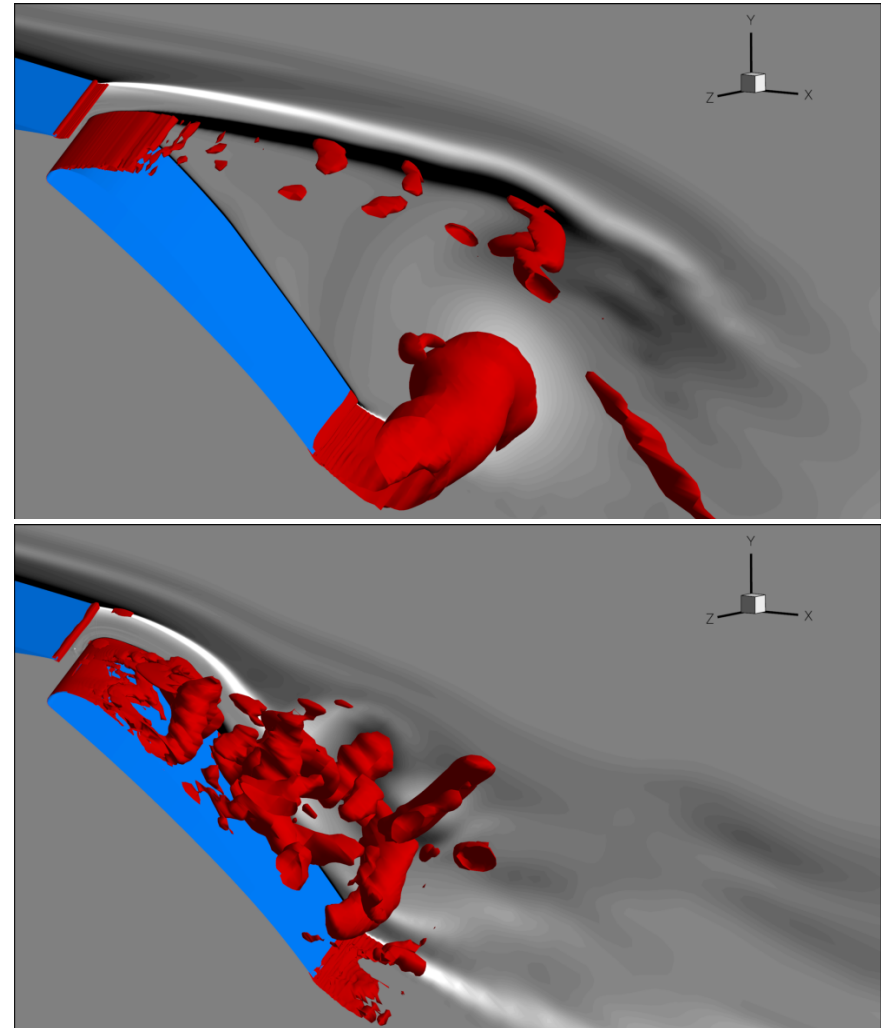
Outline

Adjoint Approaches for Optimal Active Flow Control

- **Adjoint-based sensitivity evaluation (discrete, continuous, hybrid)**
- **Automatic/Algorithmic Differentiation (AD)**
- **Comparison continuous vs. discrete adjoint for cylinder case**
- **Checkpointing for unsteady adjoint computation**
- **Sensitivity study for 3D high-lift (SCCH) test case**
- **Optimal active separation control for 2D high-lift (SCCH) test case**

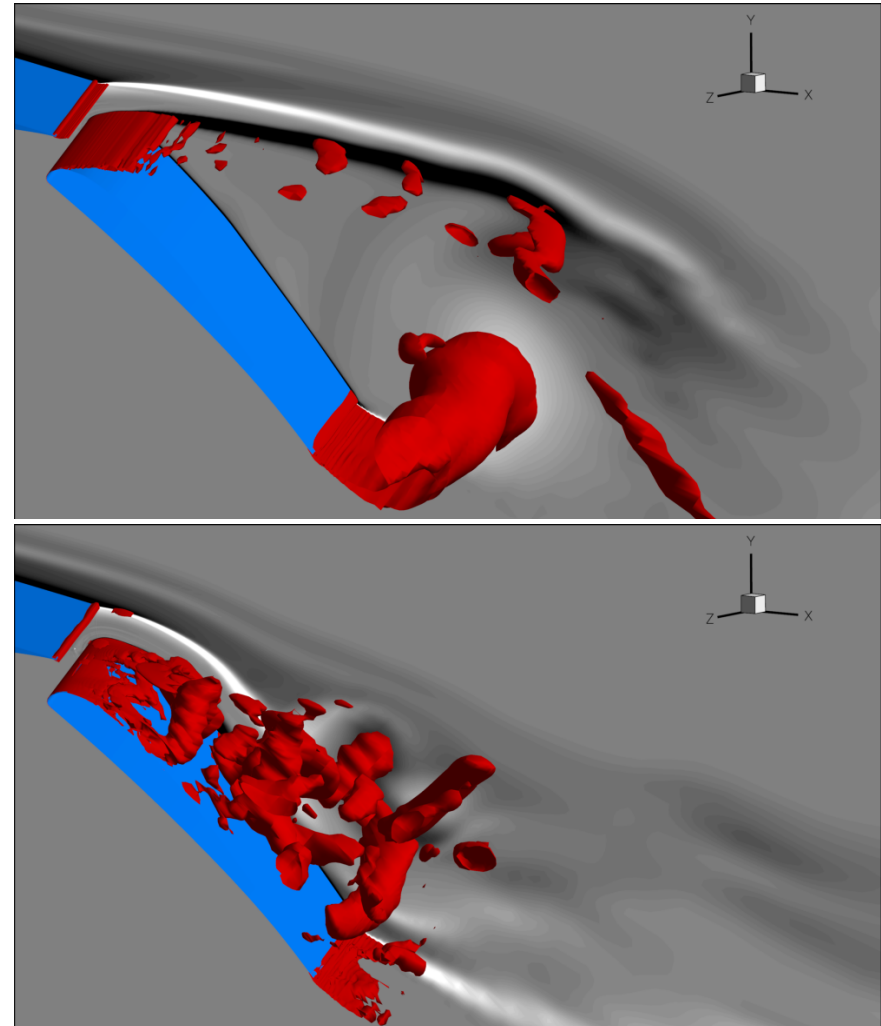
Optimal Flow Control - Motivation

- ***Aerodynamic behaviour often influenced by separation***
 - *high-lift devices*
 - *vehicles*
- ***Active flow control is promising concept to manipulate separated flow***
 - *often realised by blowing and / or suction*
- ***How to choose effective excitation parameters?***
 - *often determined by open-loop in expensive experiments / numerical simulations*



Optimal Flow Control - Motivation

- **Aerodynamic behaviour often influenced by separation**
 - *high-lift devices*
 - *vehicles*
- **Active flow control is promising concept to manipulate separated flow**
 - *often realised by blowing and / or suction*
- **How to choose effective excitation parameters?**
 - *often determined by open-loop in expensive experiments / numerical simulations*



⇒ Gradient based optimal control methods much more efficient!

Adjoint - Motivation

Optimal control problem

$$\min_{\phi \in \Phi} J(\phi, w) \quad \text{s.t.} \quad R(\phi, w) = 0$$

Gradient-based optimal control

$$\phi_{k+1} = \phi_k - \alpha_k \nabla J|_{\phi_k}$$

Calculation of the gradient

$$\nabla J|_{\phi_k} = \left(\frac{dJ}{d(\phi_k)_n} \right)_{n=1, \dots, M}$$

Finite differences

Continuous adjoint

Discrete adjoint

Adjoint - Motivation

Optimal control problem

$$\min J(\phi, w) \quad \text{s.t.} \quad R(\phi, w) = 0$$

Finite differences are inexact and too expensive to calculate

Gradients calculated by adjoints are accurate

Numerical effort for gradient computation by adjoints is independent from the number of design / control variables

⇒ Use of adjoints!

Finite differences

Continuous adjoint

Discrete adjoint

Optimality System

➤ **Optimization Problem:**

$$\min_{\phi \in \Phi} J(W, \phi) \quad s.t. \quad R(W, \phi) = 0$$

➤ **Lagrangian:**

$$L = J + \Lambda^T R$$

➤ **Optimality condition (KKT system, 1. order necessary cond.):**

$$\frac{\partial L}{\partial \Lambda} = R \stackrel{!}{=} 0 \quad \text{State equation}$$

$$\frac{\partial L}{\partial W} = \frac{\partial J}{\partial W} + \Lambda^T \frac{\partial R}{\partial W} \stackrel{!}{=} 0 \quad \text{Adjoint state equation}$$

$$\frac{\partial L}{\partial \phi} = \frac{\partial J}{\partial \phi} + \Lambda^T \frac{\partial R}{\partial \phi} \stackrel{!}{=} 0 \quad \text{Design equation}$$

Optimality System

➤ **Optimization Problem:**

$$\min_{\phi \in \Phi} J(W, \phi) \quad s.t. \quad R(W, \phi) = 0$$

➤ **Lagrangian:** instead $L = J + \Lambda^T R$, continuous L :

$$L = J + \langle \Lambda, R \rangle_{H^*, H}$$

➤ **Optimality condition (KKT system, 1. order necessary cond.):**

$$\frac{\partial L}{\partial \Lambda} = R \stackrel{!}{=} 0 \quad \text{State equation}$$

$$\frac{\partial L}{\partial W} = \frac{\partial J}{\partial W} + \Lambda^T \frac{\partial R}{\partial W} \stackrel{!}{=} 0 \quad \text{Adjoint state equation}$$

$$\frac{\partial L}{\partial \phi} = \frac{\partial J}{\partial \phi} + \Lambda^T \frac{\partial R}{\partial \phi} \stackrel{!}{=} 0 \quad \text{Design equation}$$

Optimality System

➤ **Optimization Problem:**

$$\min_{\phi \in \Phi} J(W, \phi) \quad s.t. \quad R(W, \phi) = 0 \quad \Leftrightarrow$$

Fixed point iteration:

$$W = G(W, \phi)$$

➤ **Lagrangian:** instead $L = J + \Lambda^T R$, continuous or discrete L :

$$L = J + \langle \Lambda, R \rangle_{H^*, H}$$

\Leftrightarrow

$$L(W, \Lambda, \phi) = J(W, \phi) + \Lambda^T (G(W, \phi) - W)$$

➤ **Optimality condition (KKT system, 1. order necessary cond.):**

$$\frac{\partial L}{\partial \Lambda} = R \stackrel{!}{=} 0$$

State equation

$$\frac{\partial L}{\partial W} = \frac{\partial J}{\partial W} + \Lambda^T \frac{\partial R}{\partial W} \stackrel{!}{=} 0$$

Adjoint state equation

$$\frac{\partial L}{\partial \phi} = \frac{\partial J}{\partial \phi} + \Lambda^T \frac{\partial R}{\partial \phi} \stackrel{!}{=} 0$$

Design equation

Optimality System

➤ **Optimization Problem:**

$$\min_{\phi \in \Phi} J(W, \phi) \quad s.t. \quad R(W, \phi) = 0 \quad \Leftrightarrow$$

Fixed point iteration:
 $W = G(W, \phi)$

➤ **Lagrangian:** instead $L = J + \Lambda^T R$, continuous or discrete L :

$$L = J + \langle \Lambda, R \rangle_{H^*, H}$$

\Leftrightarrow

$$L(W, \Lambda, \phi) = J(W, \phi) + \Lambda^T (G(W, \phi) - W)$$

➤ **Optimality condition (KKT system, 1. order necessary cond.):**

Black-box differentiation:

$$\frac{\partial L}{\partial \Lambda} = G(W, \phi) - W \stackrel{!}{=} 0$$

State equation

$$\frac{\partial L}{\partial W} = \frac{\partial J}{\partial W} + \Lambda^T \left(\frac{\partial G}{\partial W} - I \right) \stackrel{!}{=} 0 \Leftrightarrow N_W^T(W, \Lambda, \phi) = \Lambda$$

Adjoint state equation

$$\frac{\partial L}{\partial \phi} = \frac{\partial J}{\partial \phi} + \Lambda^T \frac{\partial G}{\partial \phi} \stackrel{!}{=} 0$$

Design equation

Optimality System

➤ **Optimization Problem:**

$$\min_{\phi \in \Phi} J(W, \phi) \quad s.t. \quad R(W, \phi) = 0 \quad \Leftrightarrow$$

Fixed point iteration:
 $W = G(W, \phi)$

➤ **Lagrangian:** instead $L = J + \Lambda^T R$, continuous or discrete L :

$$L = J + \langle \Lambda, R \rangle_{H^*, H}$$

\Leftrightarrow

$$L(W, \Lambda, \phi) = J(W, \phi) + \Lambda^T (G(W, \phi) - W)$$

Black-box differentiation:

$$G(W, \phi) - W = 0$$

$$\frac{\partial J}{\partial W} + \Lambda^T \left(\frac{\partial G}{\partial W} - I \right) = 0 \Leftrightarrow N_W^T(W, \Lambda, \phi) = \Lambda$$

Primal contractivity: $\|G_W\| = \|G_W^T\| \leq \rho < 1 \Rightarrow$ Adjoint contractivity:

Adjoint code inherits convergence properties of primal code !

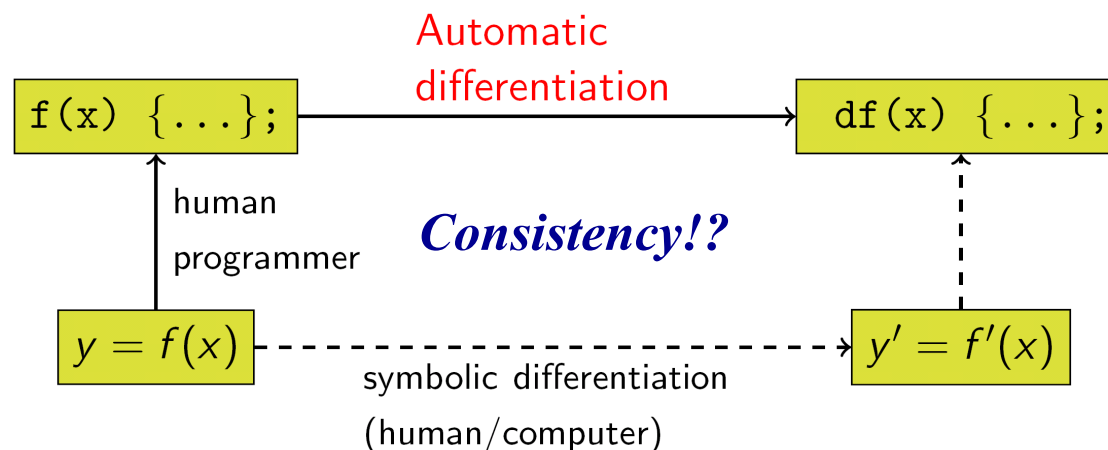
$$\left\| \frac{\partial N_W^T}{\partial \Lambda} \right\| = \|G_W^T\| \leq \rho < 1$$

Different Adjoint Approaches

- **Continuous Adjoint**
 - *optimize then discretize*
 - *hand coded adjoint solvers*
 - *time consuming in implementation*
 - *efficient in run and memory*
- **Discrete Adjoint / Algorithmic Differentiation (AD)**
 - *discretize then optimize*
 - *hand coding of adjoint solvers or ...*
 - *... more or less automated generation*
 - *memory effort increases (way out e.g. check-pointing)*
- **Hybrid Adjoint**
 - *use AD tools for parts of code*
 - *optimize differentiated code*
 - *merge “continuous and discrete” routines*

Discrete Adjoint Method

- **First discretise then optimise**
 - *First discretise the primal system*
 - *Then obtain the adjoint system based on the discretised primal equations*
- **Possibility proposed here: Automatic or Algorithmic Differentiation (AD)**
- **Basic principle**
 - *Computer code is concatenation of basic operations (+,-,*,etc.)*
 - *Apply differentiation rules to this concatenation by using chain rule*



Governing Equations

The incompressible RANS equations are given as

$$\frac{\partial(\rho \bar{u}_i)}{\partial x_i} = 0$$
$$\frac{\partial(\rho \bar{u}_i)}{\partial t} + \frac{\partial}{\partial x_i} (\rho \bar{u}_i \bar{u}_j + \overline{\rho u'_i u'_j}) = -\frac{\partial \bar{p}}{\partial x_i} + \frac{\partial \bar{\tau}_{ij}}{\partial x_i}$$

The Reynolds stresses are modeled by the eddy viscosity model

$$-\overline{\rho u'_i u'_j} = \mu_t \left(\frac{\partial \bar{u}_i}{\partial x_j} + \frac{\partial \bar{u}_j}{\partial x_i} \right) - \frac{2}{3} \rho \delta_{ij} k \quad \text{and} \quad \mu_t = 0.31 \rho k / \max(0.31 \omega; \Omega F_2)$$

Two equation SST k- ω turbulence model

$$\frac{\partial(\rho k)}{\partial t} + \frac{\partial(\rho k \bar{u}_i)}{\partial x_i} = \bar{\tau}_{ij} \frac{\partial \bar{u}_j}{\partial x_i} - \beta^* \rho \omega k + \frac{\partial}{\partial x_i} \left((\mu + \sigma_k \mu_t) \frac{\partial k}{\partial x_i} \right)$$
$$\frac{\partial(\rho \omega)}{\partial t} + \frac{\partial(\rho \omega \bar{u}_i)}{\partial x_i} = \frac{\gamma}{\nu_t} \bar{\tau}_{ij} \frac{\partial \bar{u}_j}{\partial x_i} - \beta \rho \omega^2 + \frac{\partial}{\partial x_i} \left((\mu + \sigma_\omega \mu_t) \frac{\partial \omega}{\partial x_i} \right) + 2(1 - F_1) \rho \sigma_{\omega 2} \frac{1}{\omega} \frac{\partial k}{\partial x_i} \frac{\partial \omega}{\partial x_i}$$

Governing Equations

The incompressible RANS equations are given as

$$\frac{\partial(\rho \bar{u}_i)}{\partial x_i} = 0$$

$$\frac{\partial(\rho \bar{u}_i)}{\partial t}$$

The Re

$$-\rho \overline{u'_i u'_j}$$

Two ec

$$\frac{\partial(\rho k)}{\partial t} + \frac{\partial}{\partial x_i}$$

$$\frac{\partial(\rho \omega)}{\partial t} + \frac{\partial}{\partial x_i}$$

But: $\omega \rightarrow \infty$ at wall!

\Rightarrow SST k - ω turbulence model is non-differentiable!

\Rightarrow Frozen turbulence assumption for continuous adjoint approach necessary!

\Rightarrow Leads to extra inconsistency!

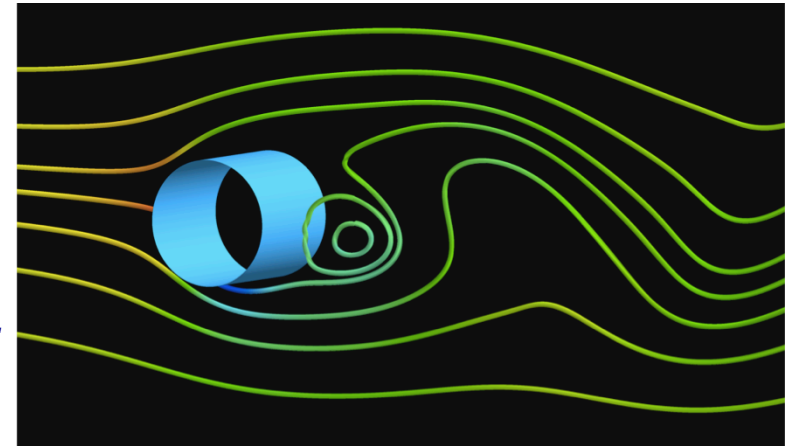
odel

$$\frac{1}{\omega} \frac{\partial k}{\partial x_i} \frac{\partial \omega}{\partial x_i}$$

Test Case and Approaches

Pre-study Continuous vs Discrete Adjoint

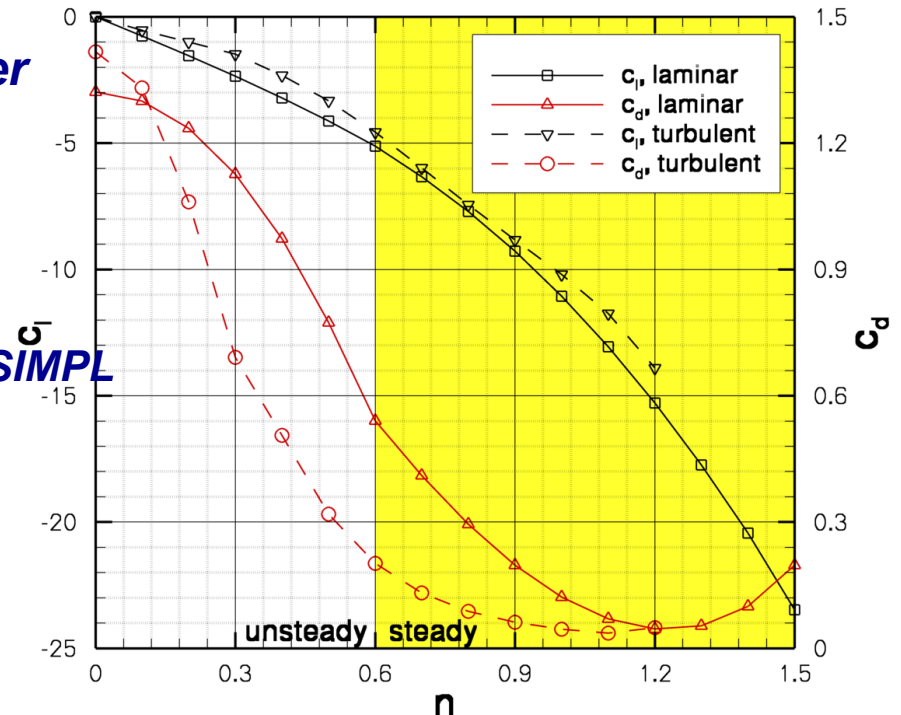
- *Drag minimisation of a rotating cylinder*
- *Control variable: Rotational speed*
- *RANS flow solver: ELAN*
 - *Block-structured, FVM, incompressible, SIMPL*
 - *Fully implicit, MPI based parallelisation*
 - *Turbulence model : SST k- ω*
 - *Coded in Fortran*
- *AD tool for adjoint : TAPENADE (INRIA Sophia – Antipolis)*
- *Reverse Accumulation for SIMPL loops [Christianson]*
- *Checkpointing by REVOLVE [Griewank, Walther]*
 - *Usable for Fortran and C*



Test Case and Approaches

Pre-study Continuous vs Discrete Adjoint

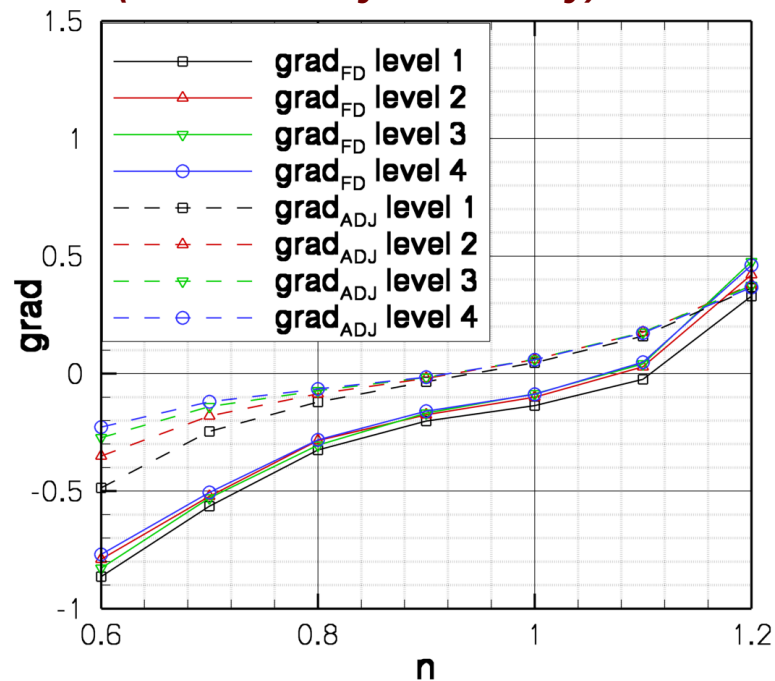
- *Drag minimisation of a rotating cylinder*
- *Control variable: Rotational speed*
- *RANS flow solver: ELAN*
 - *Block-structured, FVM, incompressible, SIMPL*
 - *Fully implicit, MPI based parallelisation*
 - *Turbulence model: SST k- ω*
 - *Coded in Fortran*
- *AD tool for adjoint: TAPENADE (INRIA Sophia – Antipolis)*
- *Reverse Accumulation for SIMPL loops [Christianson]*
- *Checkpointing by REVOLVE [Griewank, Walther]*
 - *Usable for Fortran and C*



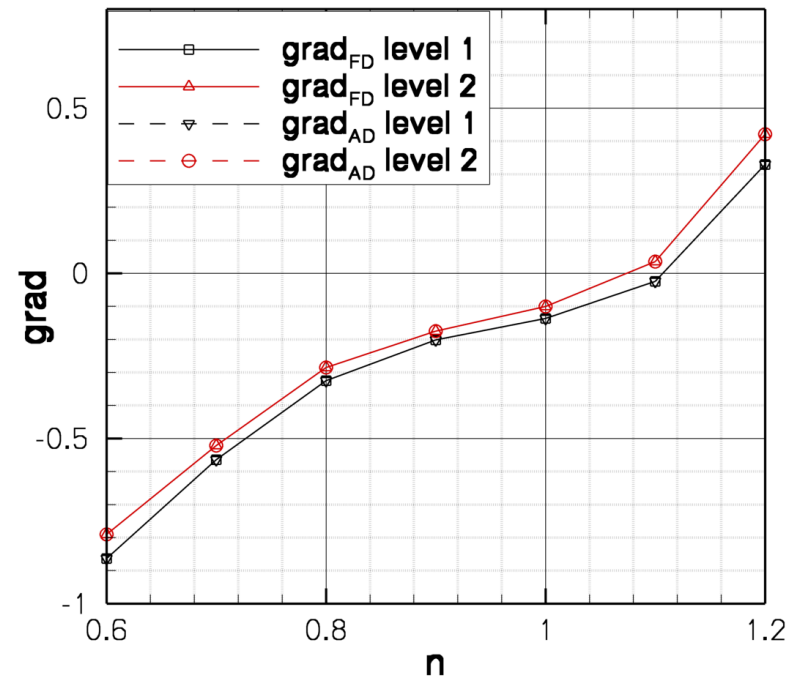
Validation of the discrete adjoint solver

- *Pre-study: Continuous vs Discrete adjoints*
- *Steady turbulent flow with $Re = 5000$*

**Continuous approach vs FD
(frozen eddy viscosity)**



**Discrete approach vs FD
(complete turbulence model)**

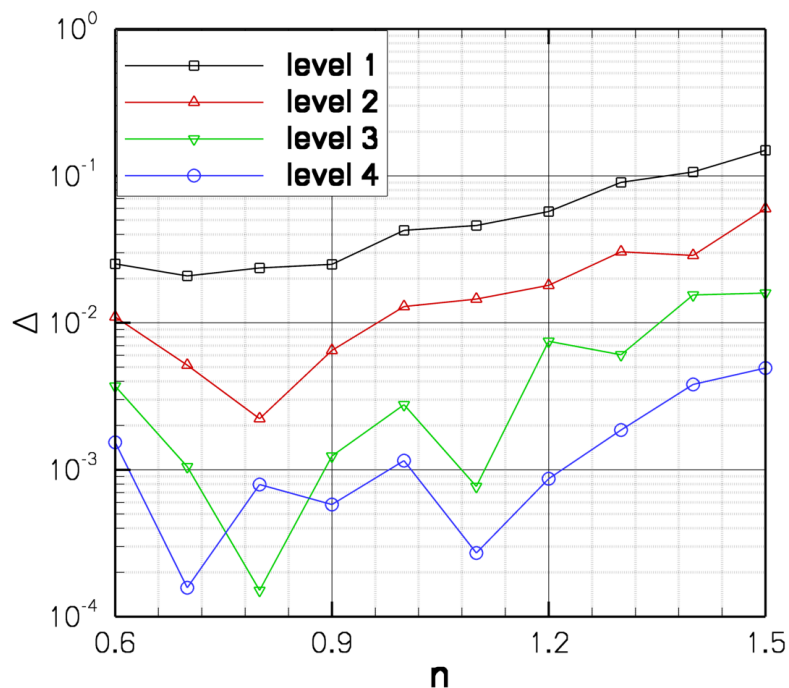


Discrete adjoints : Grid independent, more accurate and consistent
[Carnarius, Thiele, Özkaya, Gauger, AIAA-2010-5088-435, 2010]

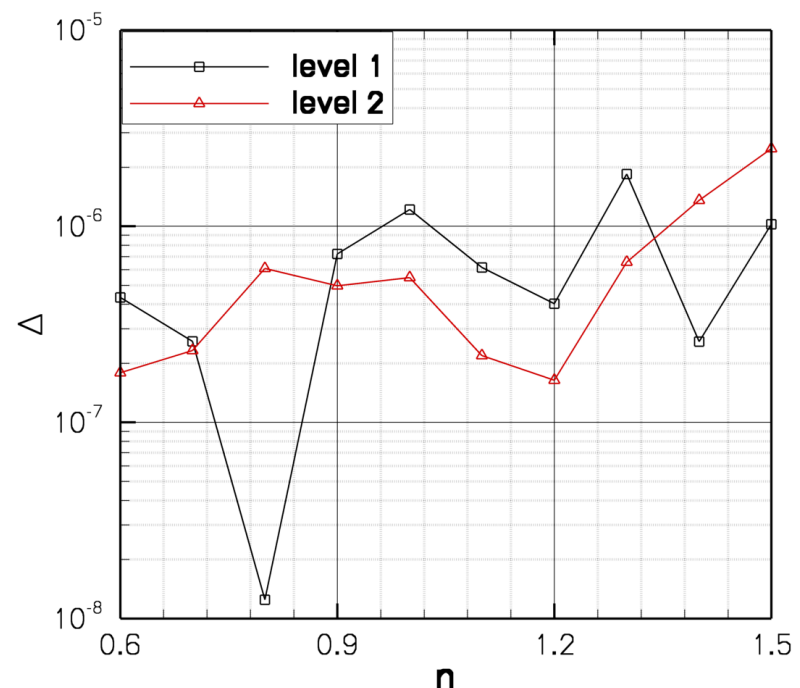
Validation of the discrete adjoint solver

- *Pre-study: Continuous vs Discrete adjoints*
- *Steady laminar flow with $Re = 100$*

Continuous approach vs FD



Discrete approach vs FD



Discrete adjoints : Grid independent, more accurate and consistent
[Carnarius, Thiele, Özkaya, Gauger, AIAA-2010-5088-435, 2010]

Development of discrete adjoint methods for unsteady optimal flow control

- Unsteady adjoint-based optimal flow control is very challenging
- Up to now not used for complex practical aerodynamic applications
- One of the main reasons is the prohibitive storage requirement as one has to store the entire flow history
- For example, the storage cost of the primal solution for a 2D URANS incompressible solver with 10^5 grid points and 1000 unsteady time iterations is $O(10)$ Gb
- Obviously, for practical complex configurations in 3D with more number of grid points and time iterations, the storage requirements may become prohibitively large

Exact and approximate approaches

Several strategies have been proposed to circumvent the memory requirements

Exact methods

- *Store all in hard disk approach*
- *Use of checkpoints*
- *...*

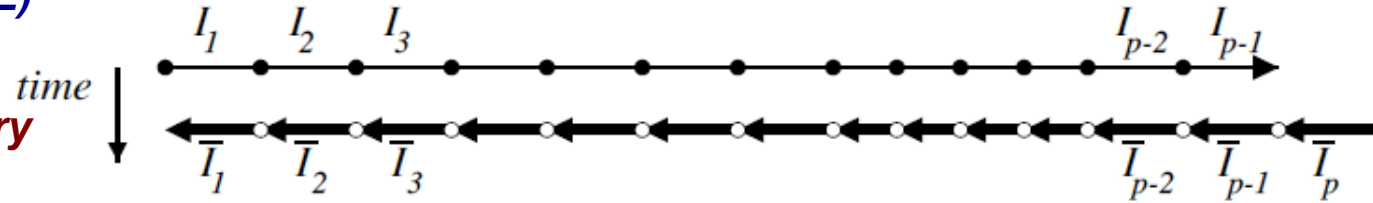
Approximate methods

- *Reduced order methods (e.g. POD models)*
- *Non-linear frequency domain methods*
- *...*

Checkpointing

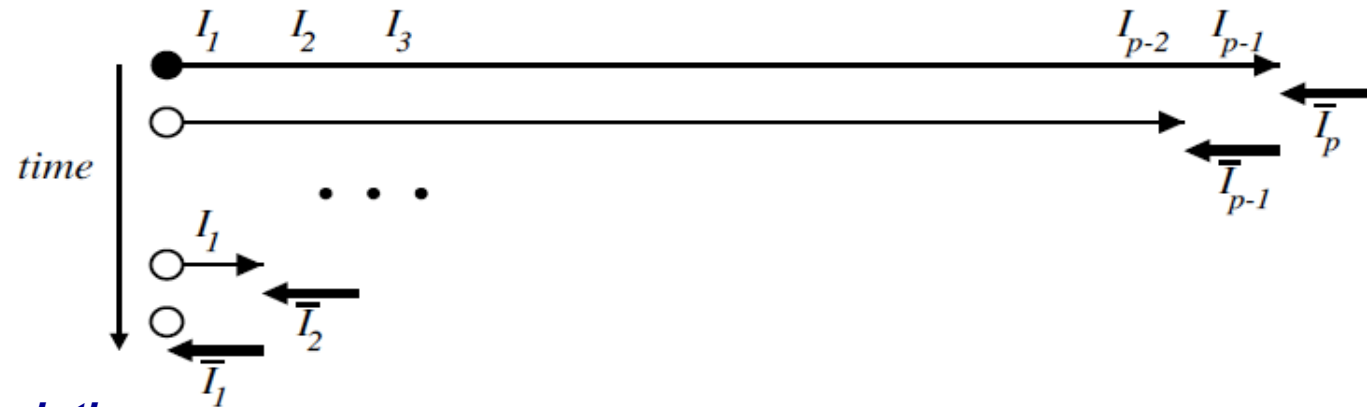
Store-All (TAPENADE)

Excessive memory requirements

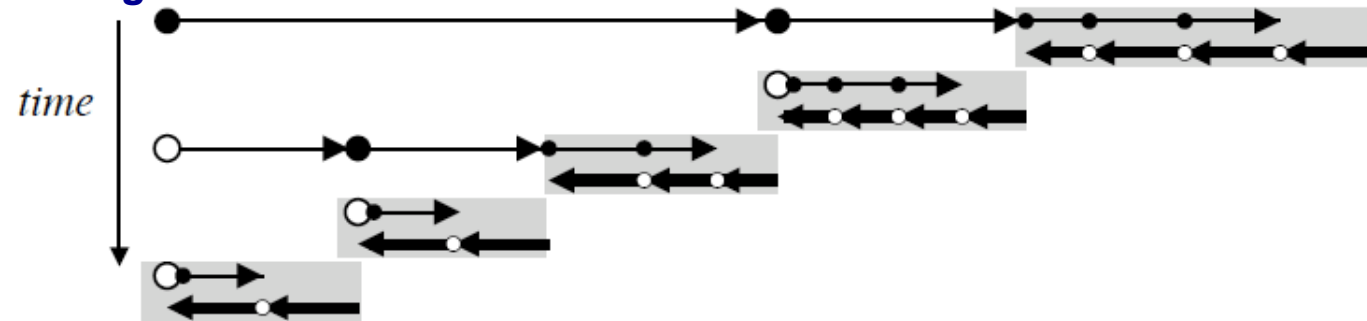


Recompute-All (TAF)

Excessive CPU requirements



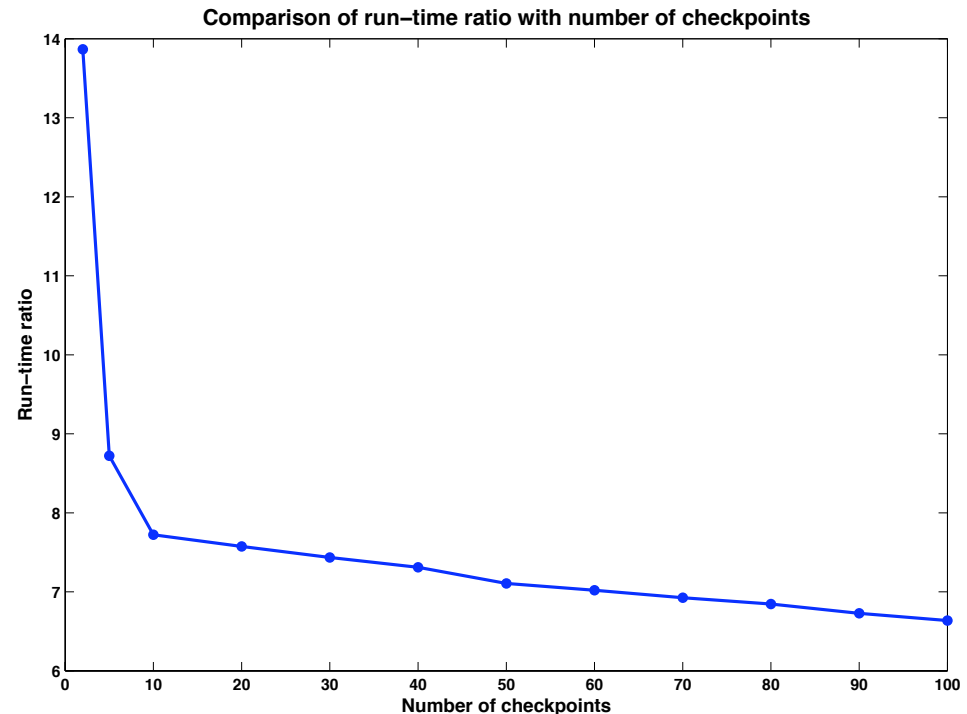
Compromise: Checkpointing



Variation of run time ratio with checkpoints

Unsteady time steps = 100

$$\text{Run time ratio} = \frac{T(\text{adjoint})}{T(\text{primal})}$$

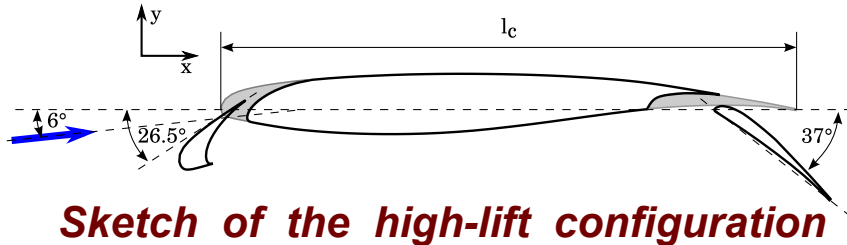


Comments on checkpointing approach :

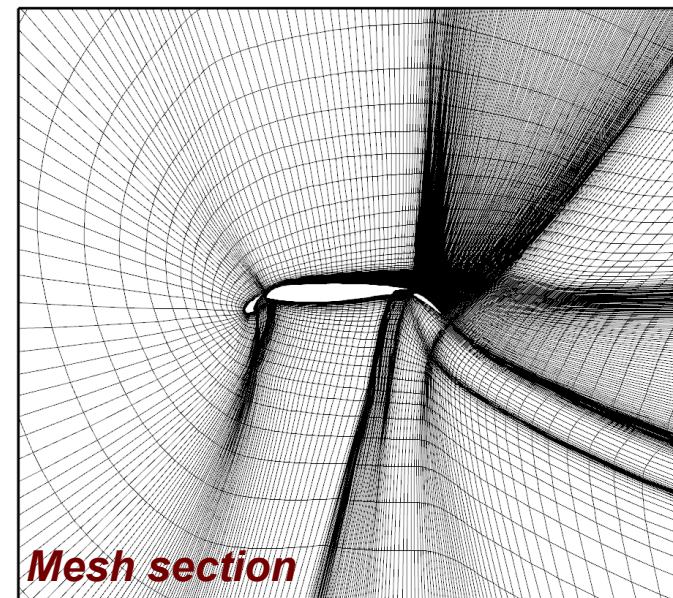
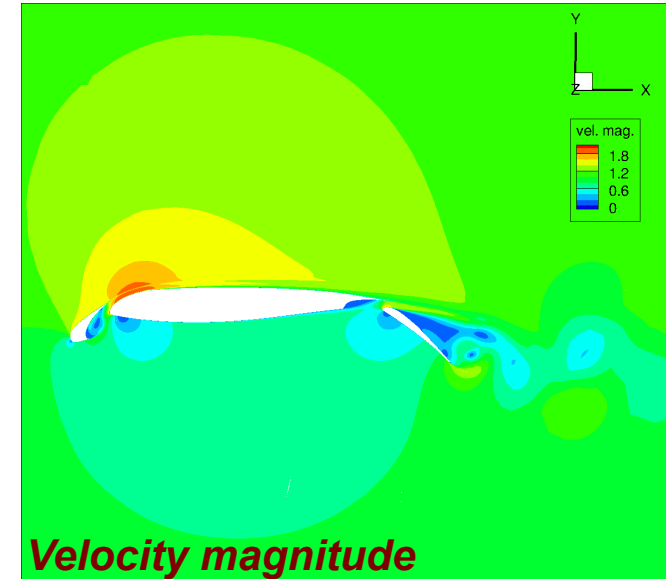
- *Significantly reduces the memory*
- *Increases the run time due to extra flow calculations*
- *Binomial checkpointing ensures optimal extra flow computations*

3D High-Lift (SCCH) Test Case

Turbulent flow, $Re=10^6$, $\alpha=6^\circ$



- Lift maximization of a 3D high-lift configuration using sinusoidal blowing and suction type of actuation with zero net mass flux
- $Re = 10^6$ and $AoA = 6^\circ$
- Turbulence model: SST k-w
- 689,568 finite volumes
- 3D grid generated by stacking 16 layers of 2D grid along spanwise direction and applying respective sweep angle



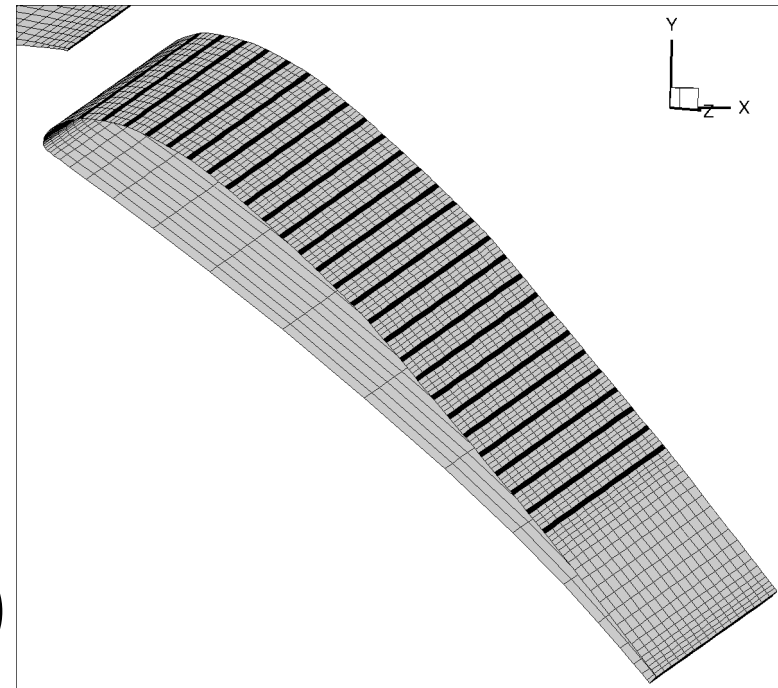
3D High-Lift (SCCH) Test Case

Turbulent flow, $Re=10^6$, $\alpha=6^\circ$

Lift maximization using actuation:

- 27 actuation faces along suction side
- No. of actuation faces = $27 \times 16 = 432$
- The actuation boundary condition at a slot face is given by

$$\begin{pmatrix} u \\ v \\ w \end{pmatrix} = A \left[\vec{n} + \frac{1}{\tan \beta_1} \vec{t}_1 + \frac{1}{\tan \beta_2} \vec{t}_2 \right] \cos(2\pi f(t - t_0))$$



Actuation slots on the flap

Objective function:

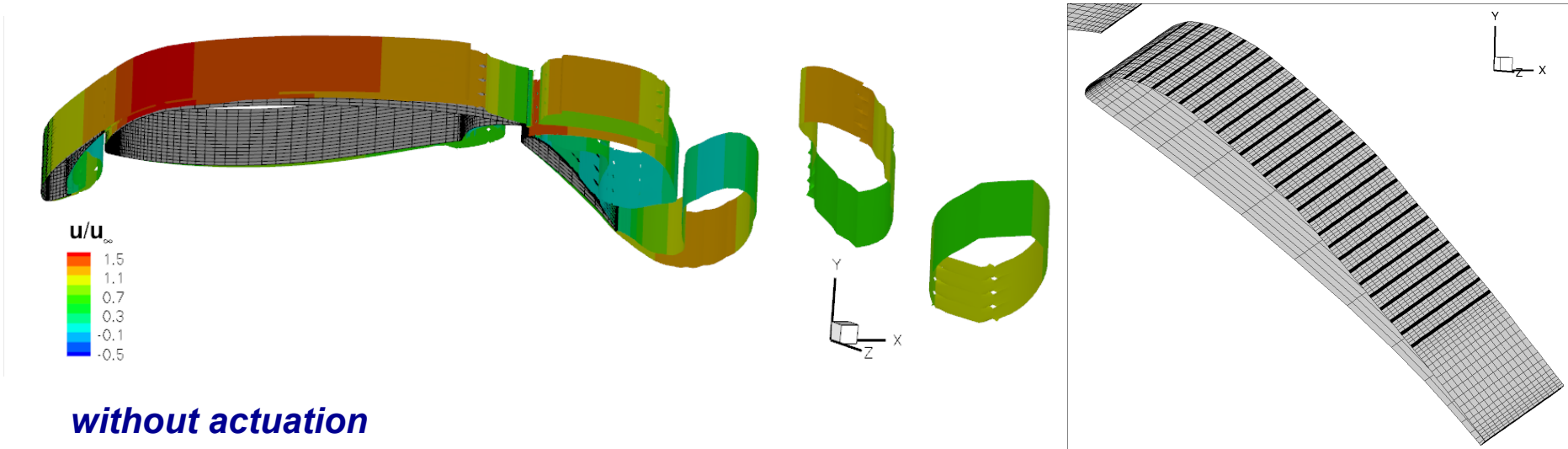
$$J = \bar{C}_l = \frac{1}{500} \sum_{n=1}^{500} C_l^n$$

Control variables:

$$\begin{pmatrix} A - \text{Amplitude} \\ \beta_{1,2} - \text{Angles} \\ t_0 - \text{Phase shift} \end{pmatrix} = 1728$$

3D High-Lift (SCCH) Test Case

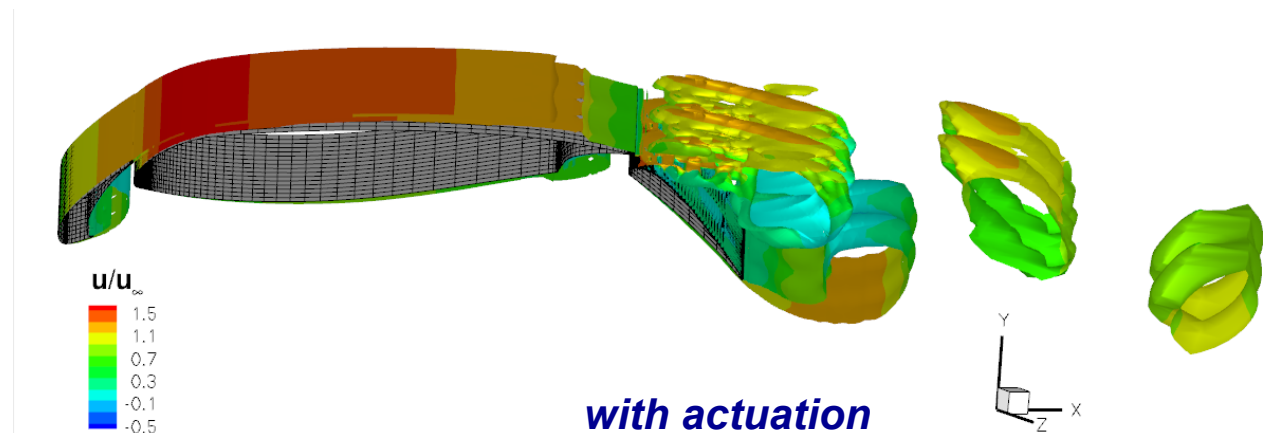
Turbulent flow, $Re=10^6$, $\alpha=6^\circ$



without actuation

Iso-surfaces of the vortex indicator

Actuation slots on the flap



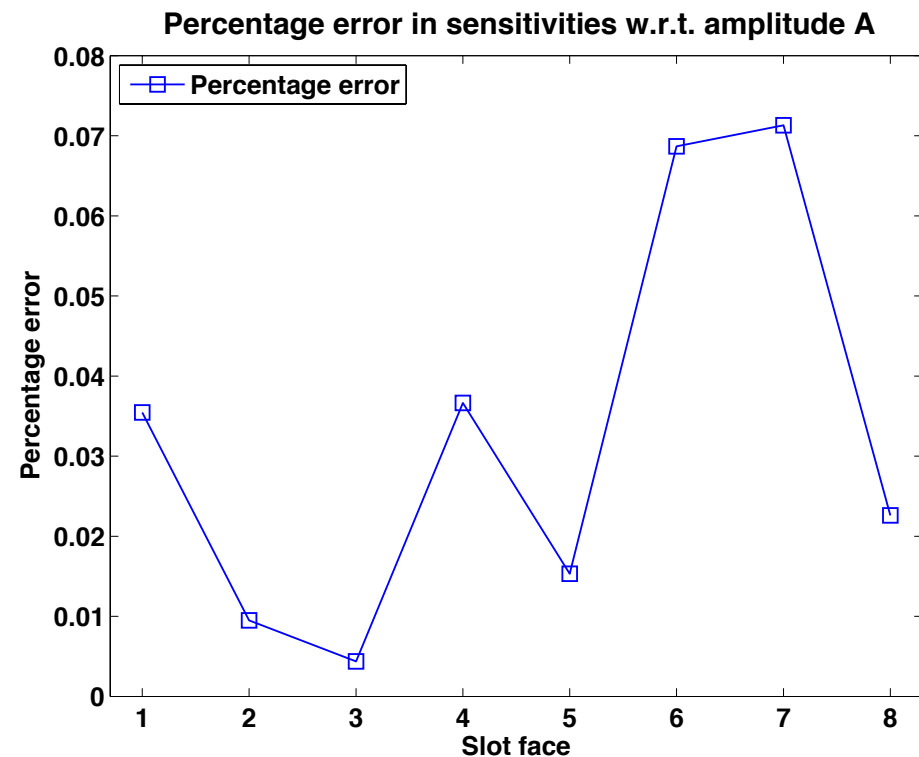
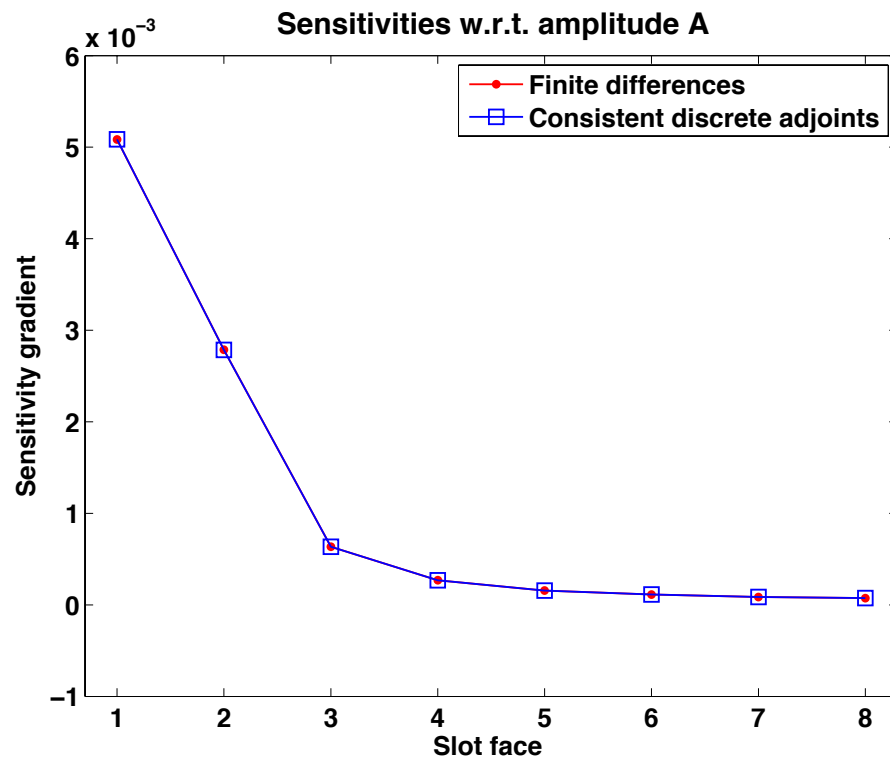
with actuation

3D High-Lift (SCCH) Test Case

Turbulent flow, $Re=10^6$, $\alpha=6^\circ$

Comparison of sensitivity gradients

Consistent discrete adjoints VS. 2nd Order finite differences



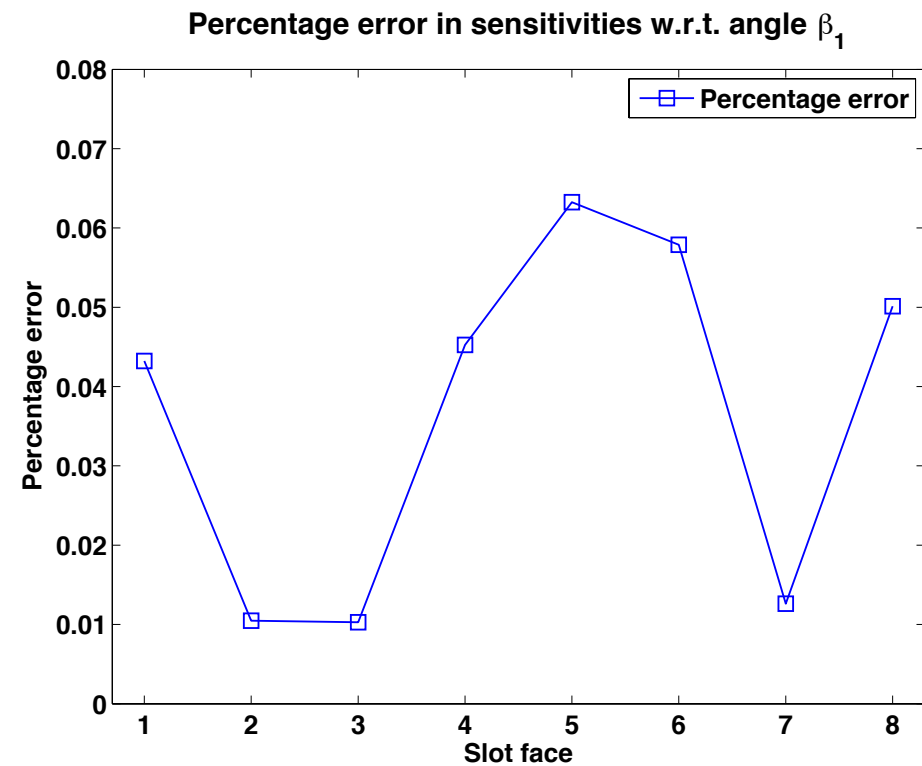
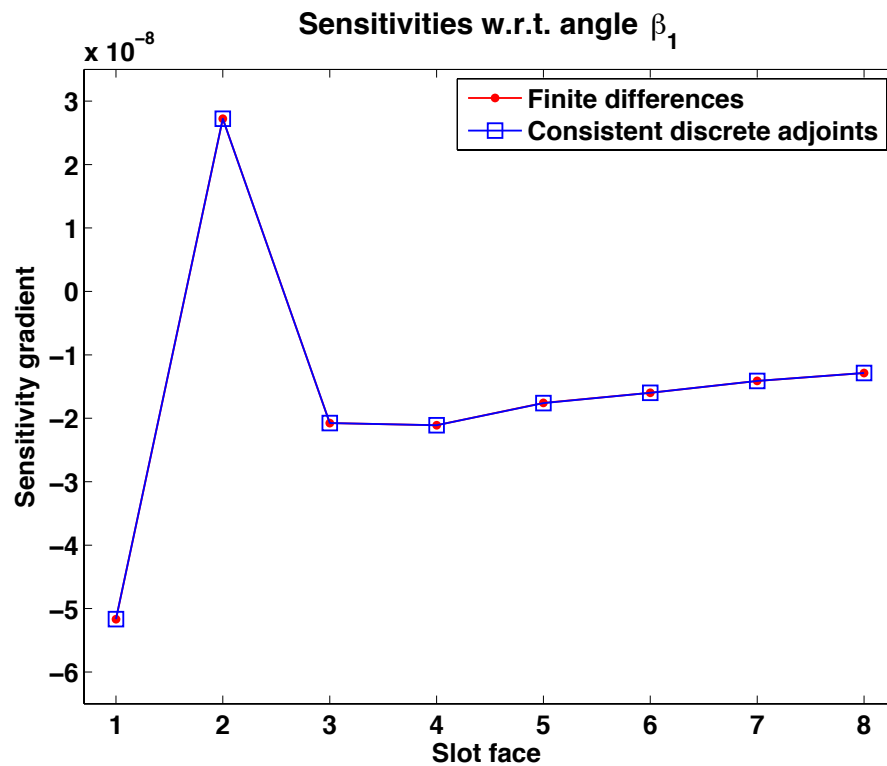
Amplitude sensitivities at 8 randomly selected actuation faces

3D High-Lift (SCCH) Test Case

Turbulent flow, $Re=10^6$, $\alpha=6^\circ$

Comparison of sensitivity gradients

Consistent discrete adjoints VS. 2nd Order finite differences



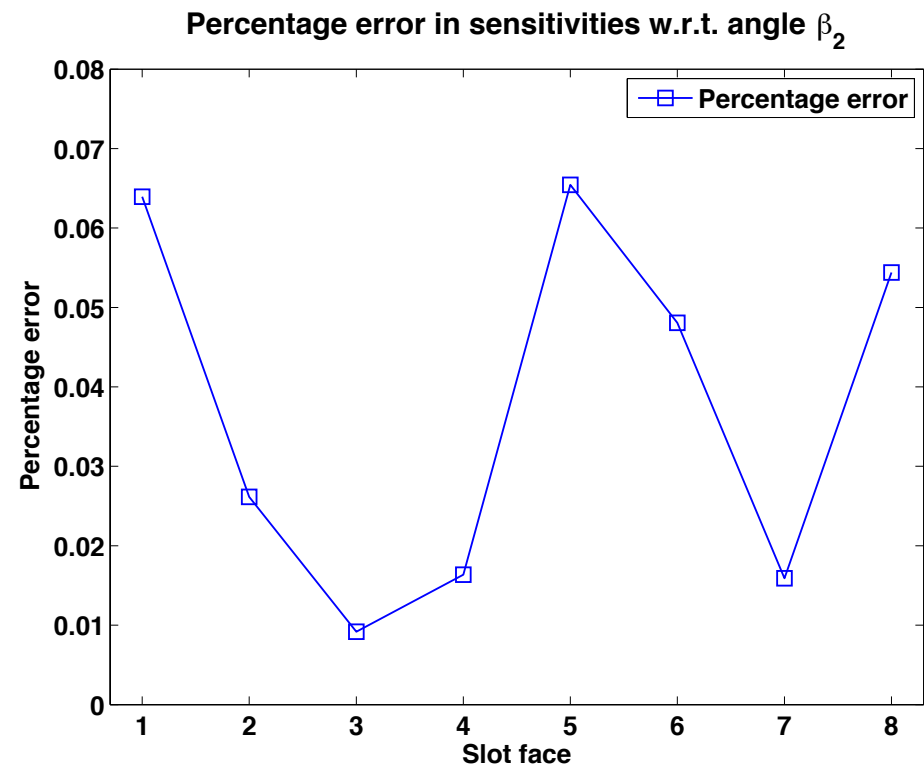
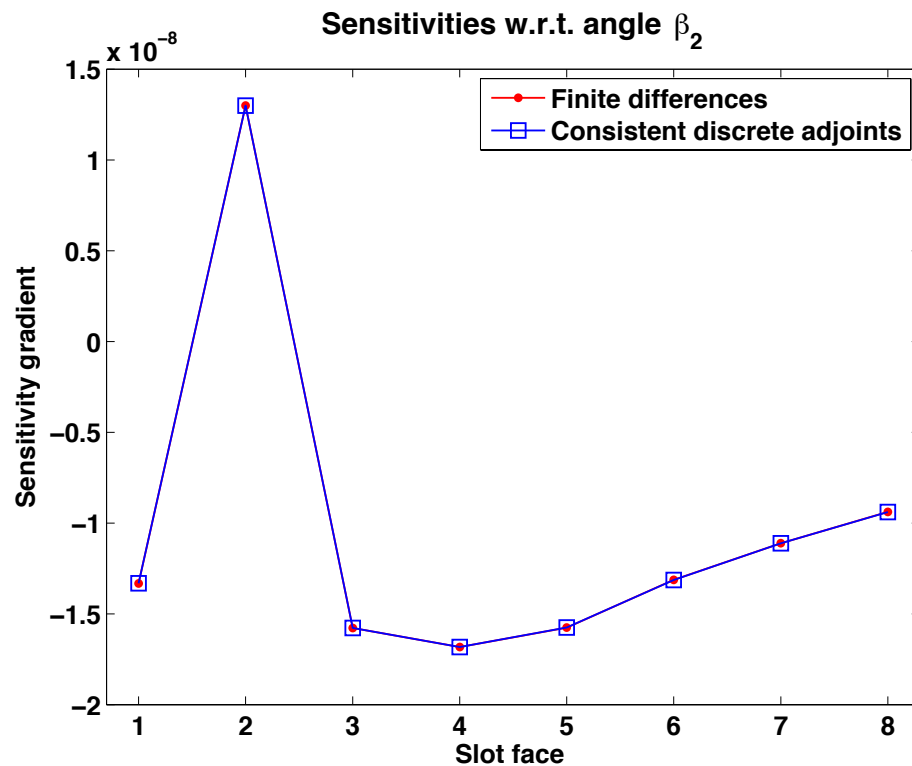
Angle β_1 sensitivities at 8 randomly selected actuation faces

3D High-Lift (SCCH) Test Case

Turbulent flow, $Re=10^6$, $\alpha=6^\circ$

Comparison of sensitivity gradients

Consistent discrete adjoints VS. 2nd Order finite differences



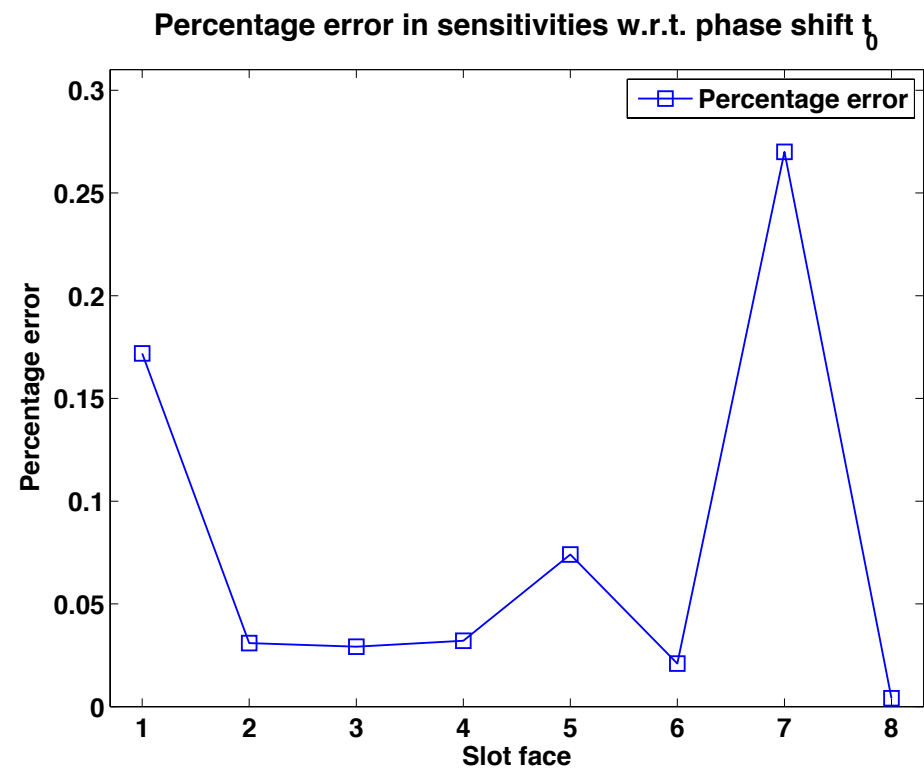
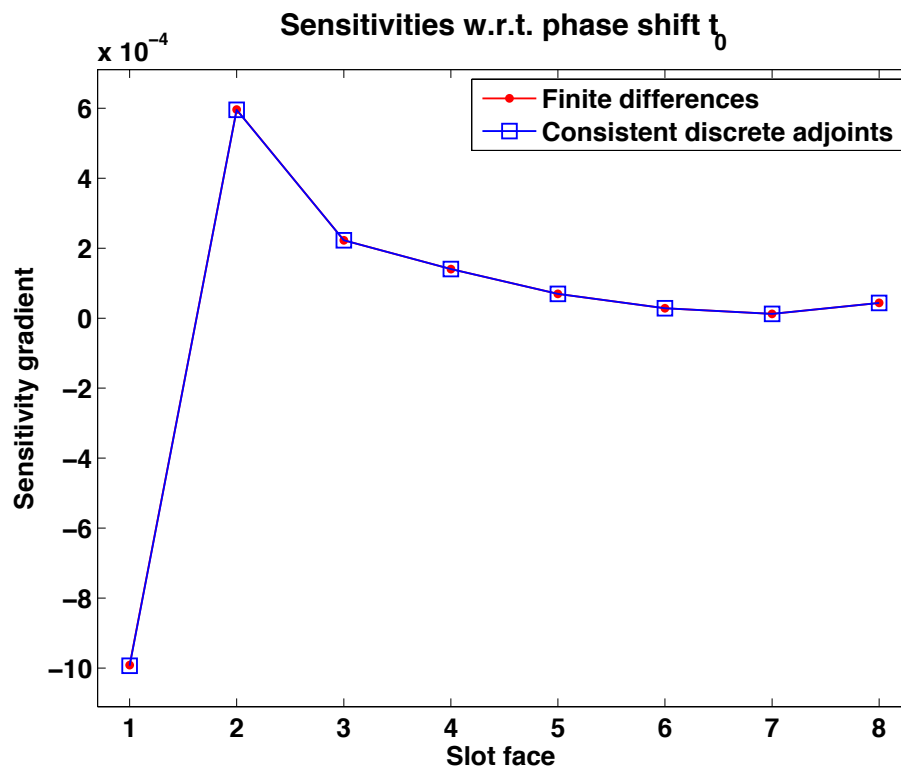
Angle β_2 sensitivities at 8 randomly selected actuation faces

3D High-Lift (SCCH) Test Case

Turbulent flow, $Re=10^6$, $\alpha=6^\circ$

Comparison of sensitivity gradients

Consistent discrete adjoints VS. 2nd Order finite differences



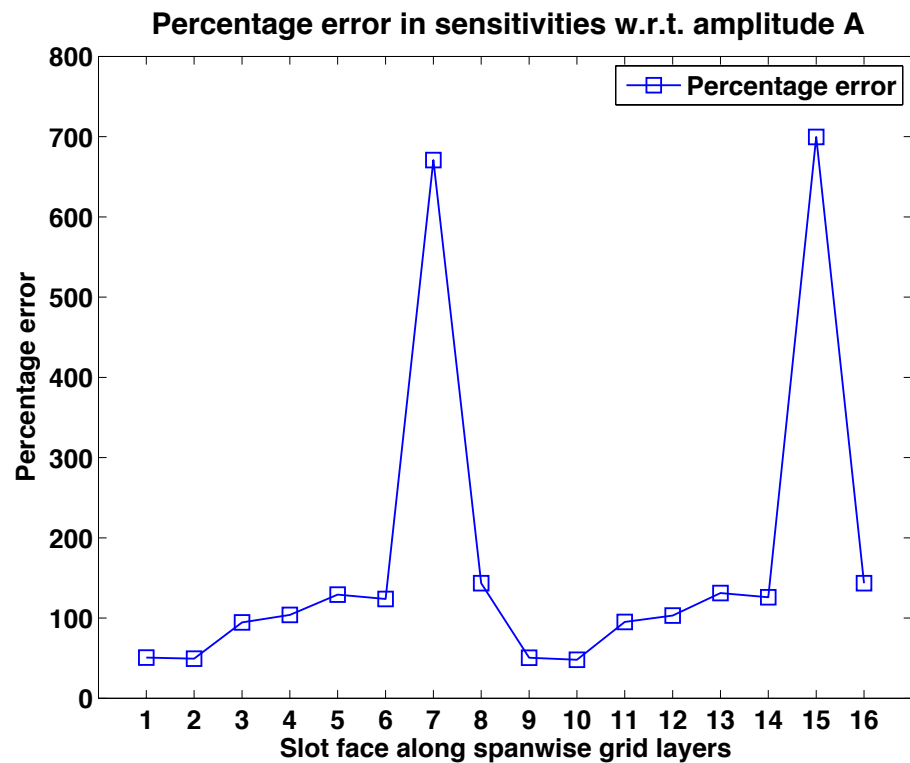
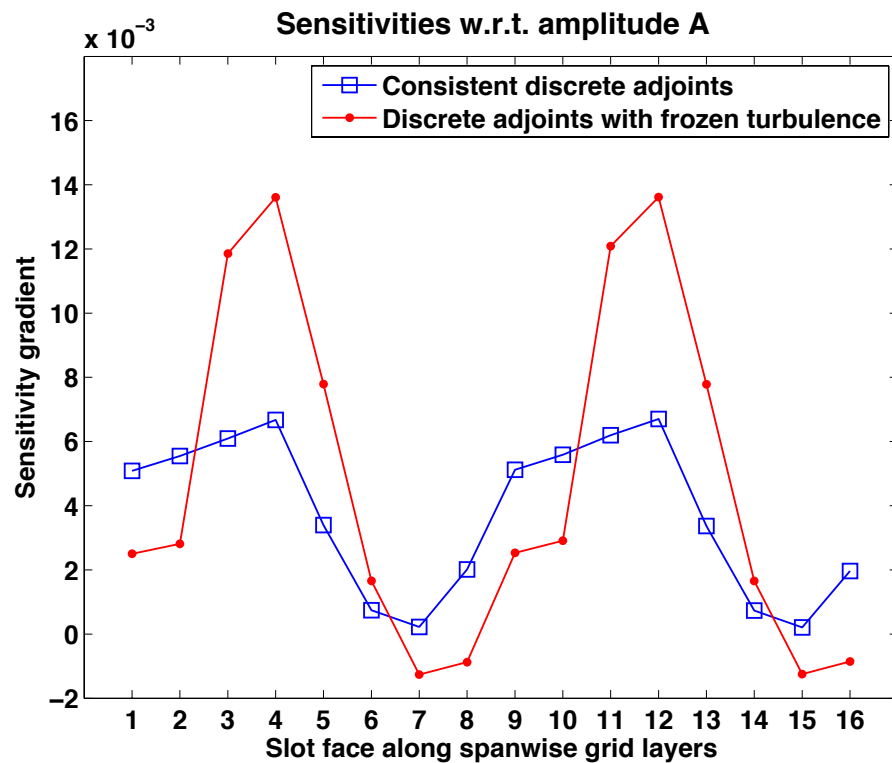
Phase shift sensitivities at 8 randomly selected actuation faces

3D High-Lift (SCCH) Test Case

Turbulent flow, $Re=10^6$, $\alpha=6^\circ$

Comparison of sensitivity gradients

Consistent discrete adjoints VS. Discrete adjoints with frozen turbulence assumption



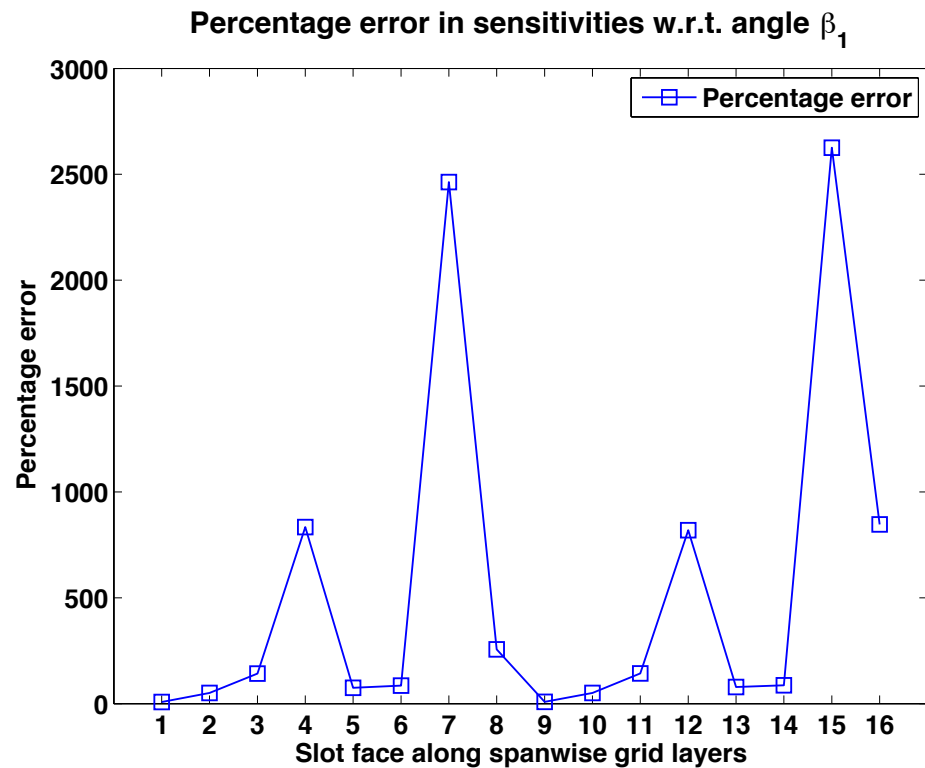
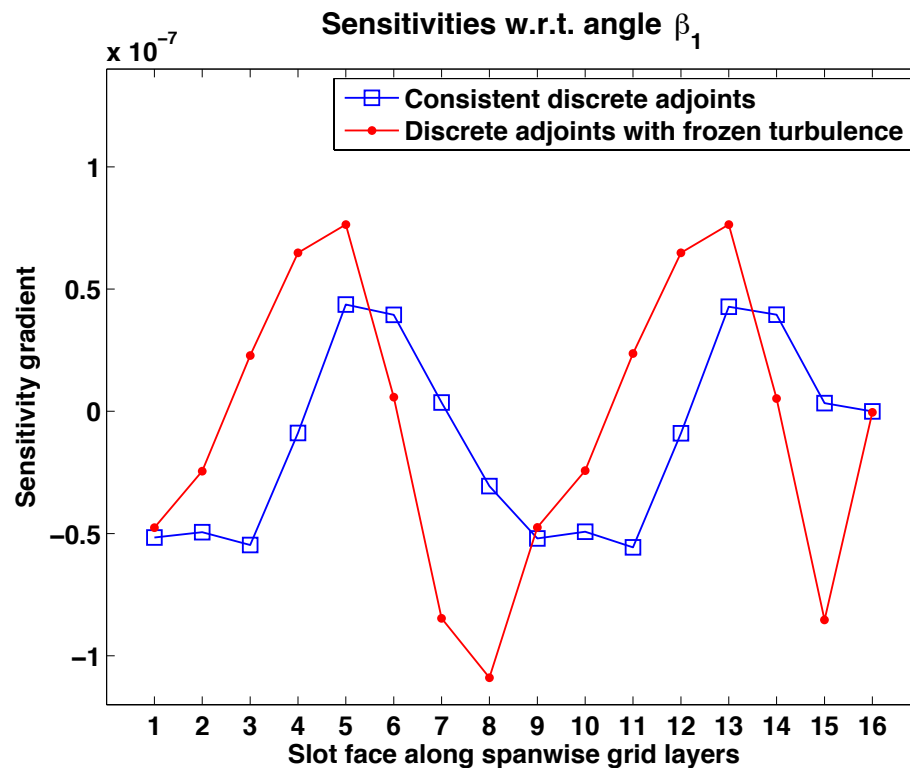
Amplitude sensitivities at all 16 slot faces along the spanwise grid layers

3D High-Lift (SCCH) Test Case

Turbulent flow, $Re=10^6$, $\alpha=6^\circ$

Comparison of sensitivity gradients

Consistent discrete adjoints VS. Discrete adjoints with frozen turbulence assumption



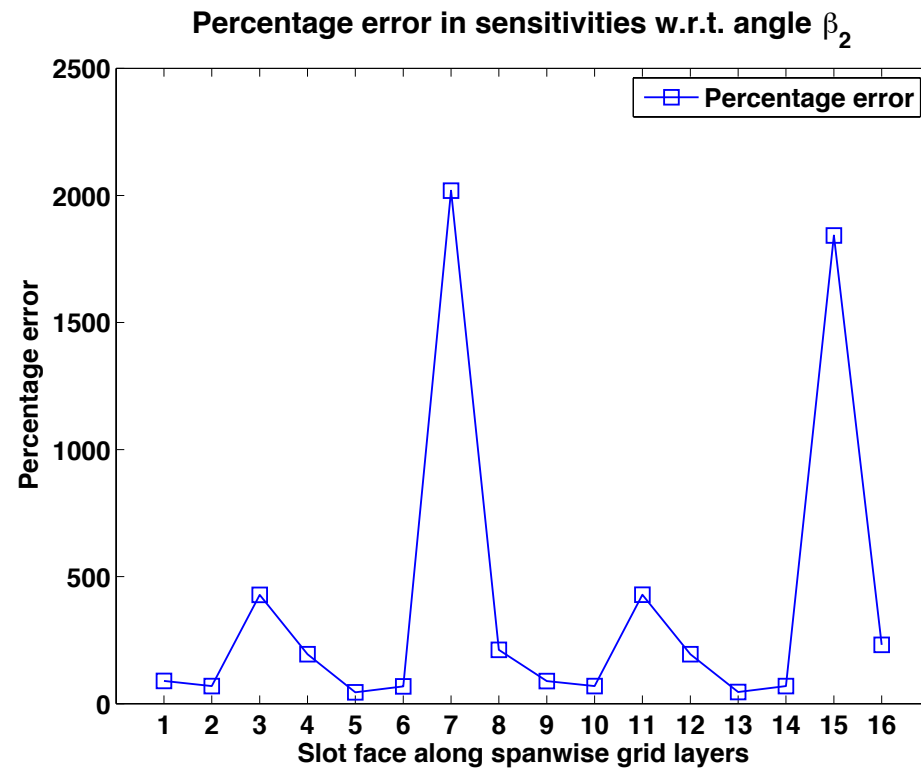
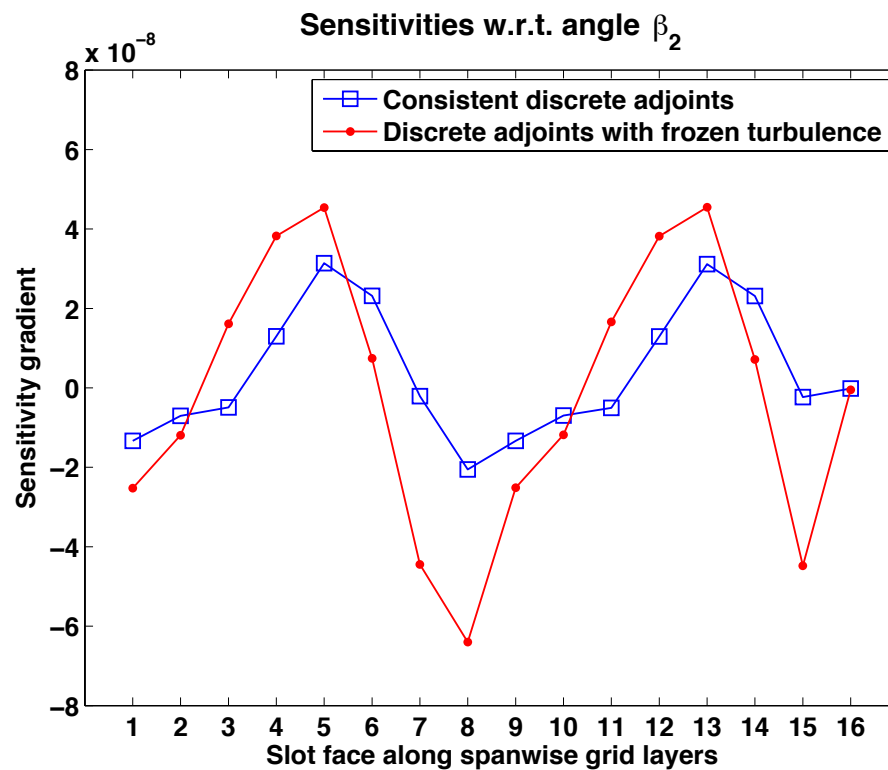
Angle β_1 sensitivities at all 16 slot faces along the spanwise grid layers

3D High-Lift (SCCH) Test Case

Turbulent flow, $Re=10^6$, $\alpha=6^\circ$

Comparison of sensitivity gradients

Consistent discrete adjoints VS. Discrete adjoints with frozen turbulence assumption



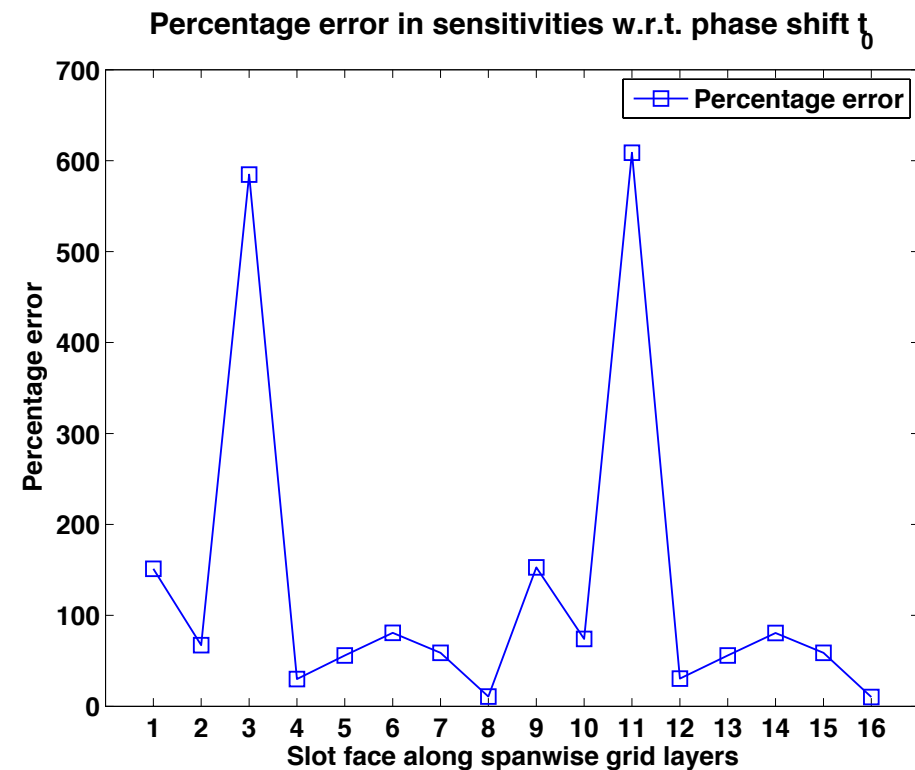
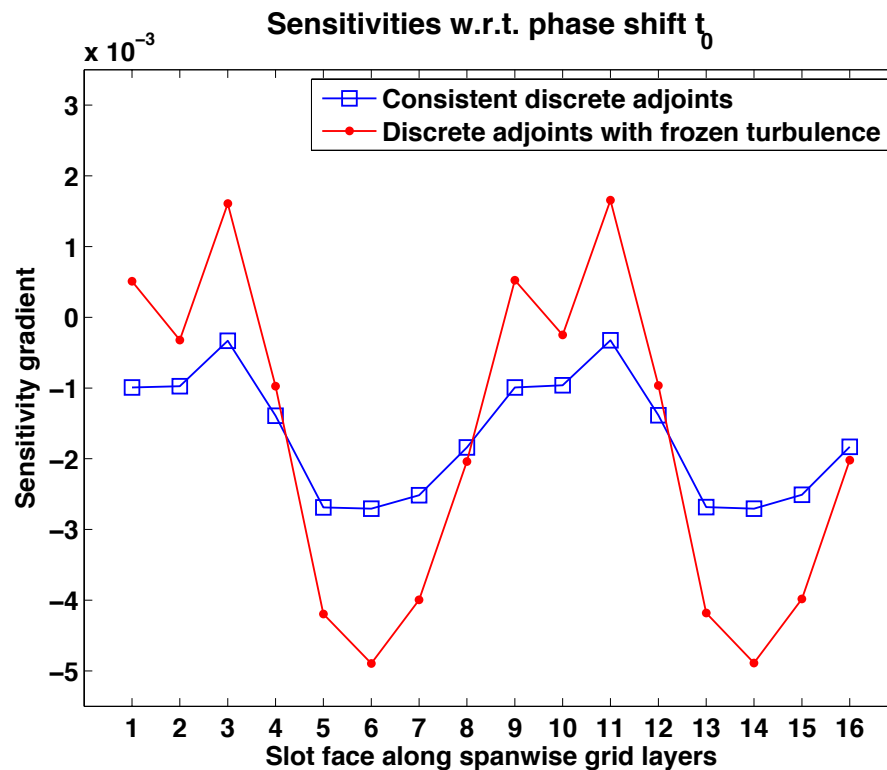
Angle β_2 sensitivities at all 16 slot faces along the spanwise grid layers

3D High-Lift (SCCH) Test Case

Turbulent flow, $Re=10^6$, $\alpha=6^\circ$

Comparison of sensitivity gradients

Consistent discrete adjoints VS. Discrete adjoints with frozen turbulence assumption

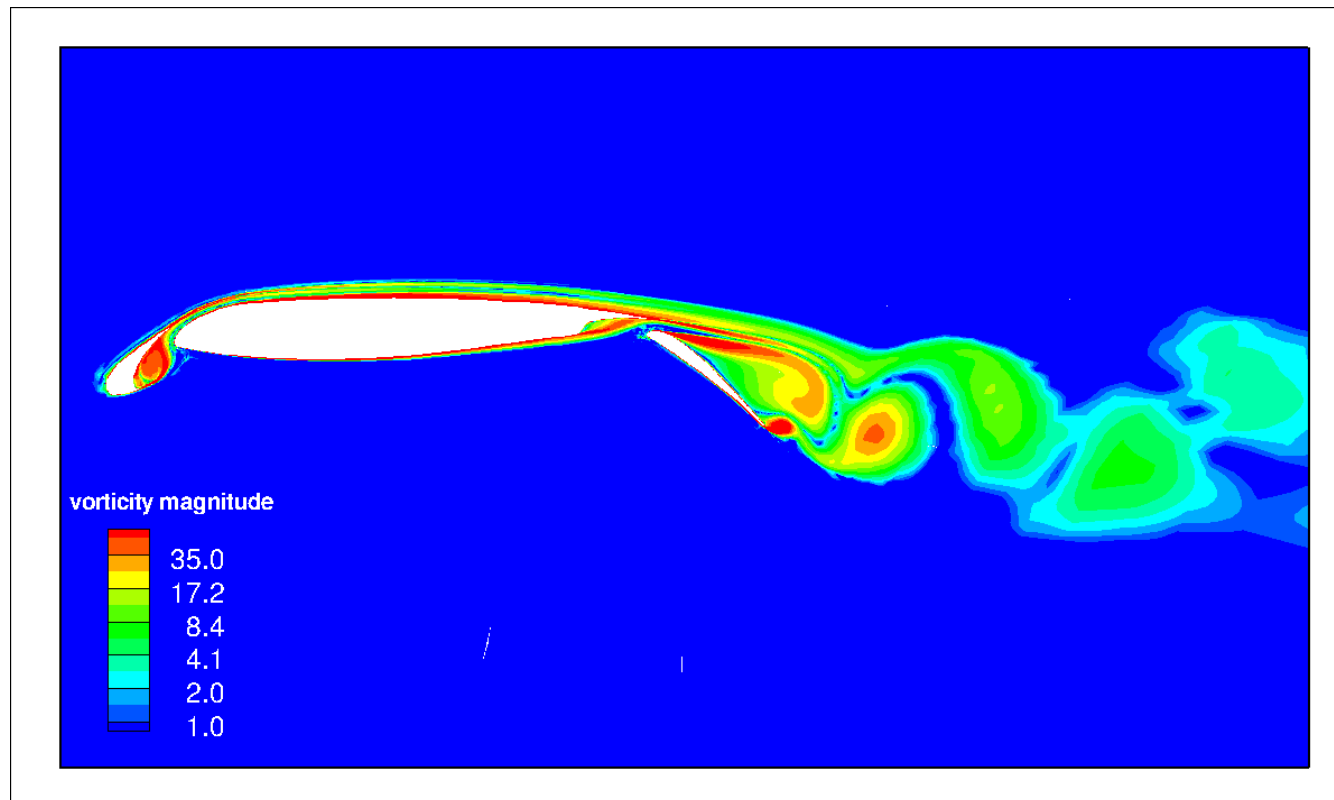


Phase shift sensitivities at all 16 slot faces along the spanwise grid layers

2D SCCH High-Lift Configuration

Turbulent flow, $Re=10^6$, $\alpha=6^\circ$

Un-actuated flow



Contours of vorticity magnitude

2D SCCH High-Lift Configuration

Turbulent flow, $Re=10^6$, $\alpha=6^\circ$

Lift maximisation using active flow control:

- A cascade of 27 actuation slits is installed on the suction side of the flap
- The synthetic jet actuation boundary condition at a slit face is given by

$$\begin{pmatrix} u^k \\ v^k \end{pmatrix} = A^k \begin{pmatrix} \frac{\cos \theta}{\tan \beta^k} - \sin \theta \\ \frac{\sin \theta}{\tan \beta^k} + \cos \theta \end{pmatrix} \sin [2\pi f (t - t_0^k)]$$

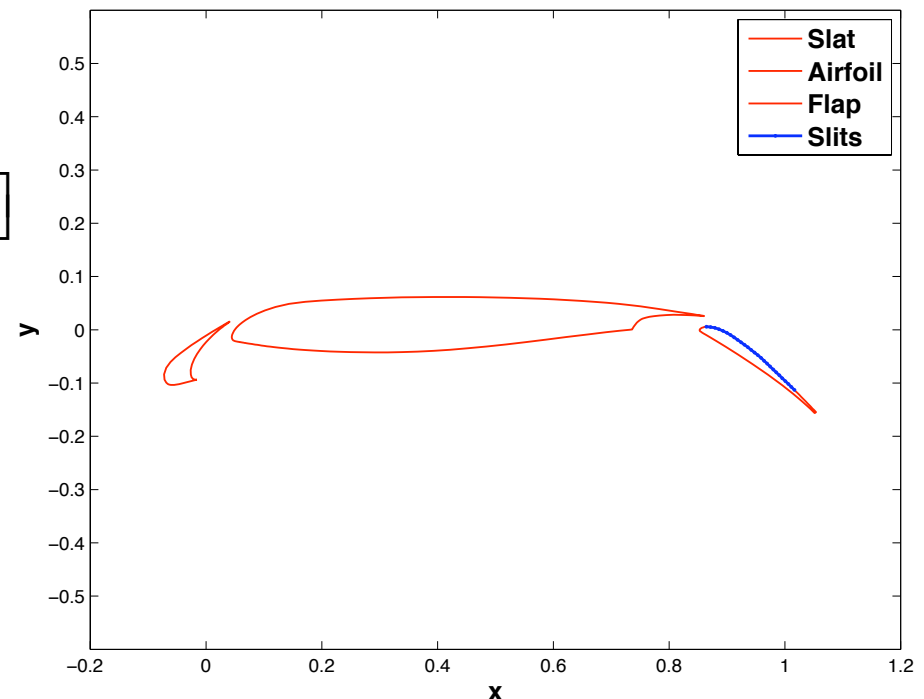
A^k – Amplitude

t_0^k – Phase shift

β^k – Angle

k – Slit index ($k = 1, \dots, 27$)

Slit locations on the flap



2D SCCH High-Lift Configuration

Turbulent flow, $Re=10^6$, $\alpha=6^\circ$

Lift maximisation using active flow control:

- A cascade of 27 actuation slits is installed on the suction side of the flap
- The actuation boundary condition at a slit face is given by

$$\begin{pmatrix} u^k \\ v^k \end{pmatrix} = A^k \begin{pmatrix} \frac{\cos \theta}{\tan \beta^k} - \sin \theta \\ \frac{\sin \theta}{\tan \beta^k} + \cos \theta \end{pmatrix} \sin [2\pi f (t - t_0^k)]$$

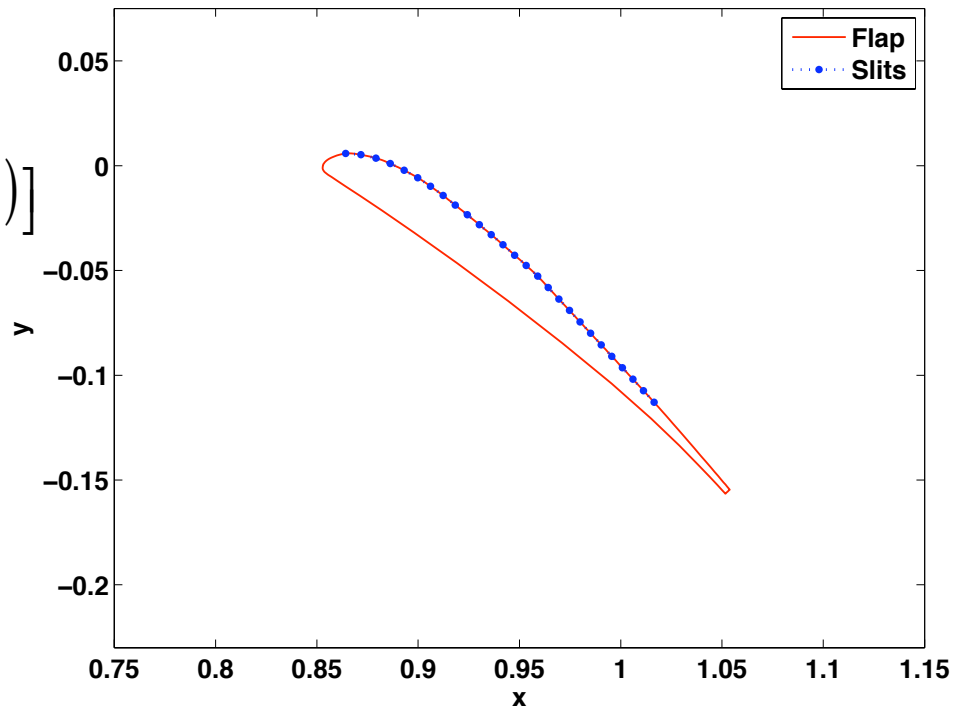
A^k – Amplitude

t_0^k – Phase shift

β^k – Angle

k – Slit index ($k = 1, \dots, 27$)

Slit locations on the flap



2D SCCH High-Lift Configuration

Turbulent flow, $Re=10^6$, $\alpha=6^\circ$

Optimal active flow control:

Objective function: Mean lift

$$J = \bar{C}_l = \frac{1}{N - N^*} \sum_{n=N^*+1}^N C_l^n$$

Time interval: $[0, T] = [0, 30]$

$$\Delta t = 0.002$$

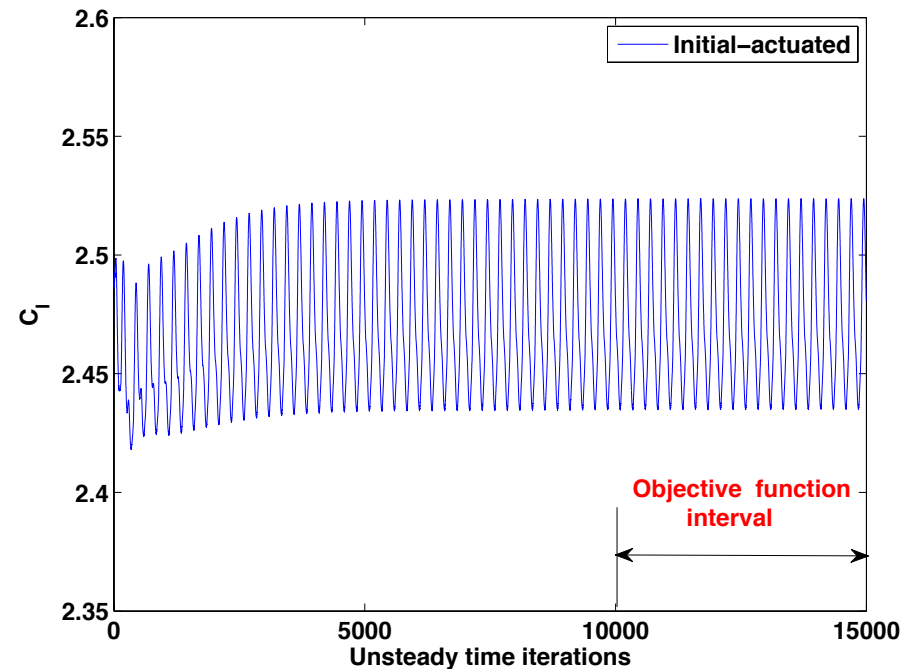
$$T = N \cdot \Delta t$$

$$N = 15000, N^* = 10000$$

Control variables:

$$\begin{pmatrix} A^k & - \text{Amplitude} \\ t_0^k & - \text{Phase shift} \\ \beta^k & - \text{Angle} \end{pmatrix} = 81$$

Turbulence model: SST $k-\omega$



Initial actuated flow

$$A^k = 0.3, \beta^k = 90^\circ, t_0^k = -0.125$$

2D SCCH High-Lift Configuration

Turbulent flow, $Re=10^6$, $\alpha=6^\circ$

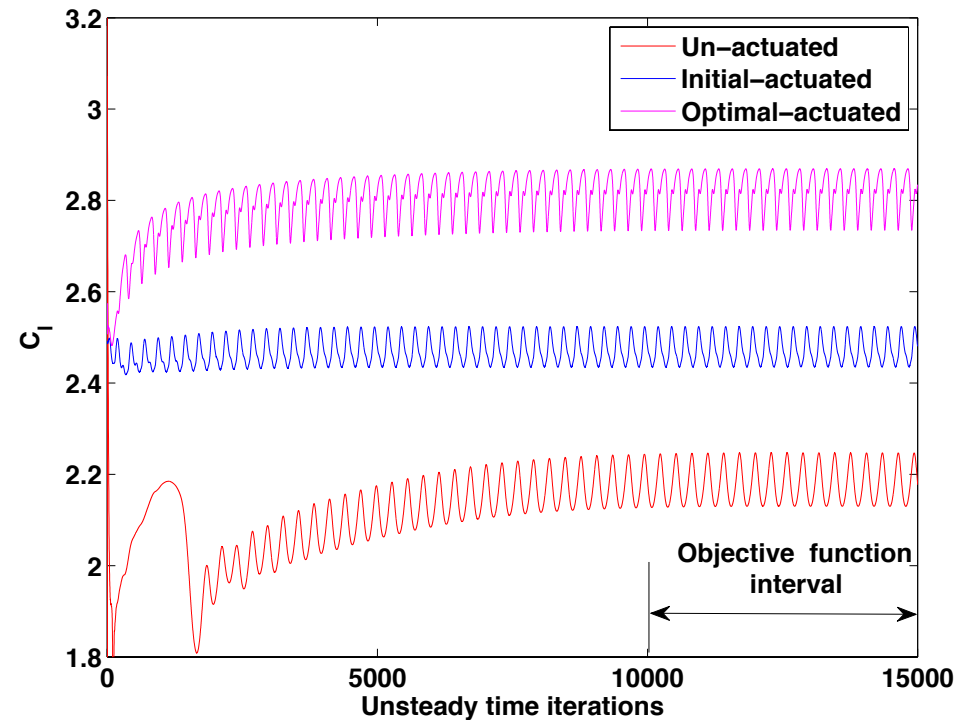
Optimal active flow control:

Optimiser: BFGS Quasi Newton Algorithm

Un-actuated flow : $\bar{C}_l = 2.1802$

Initial actuated flow : $\bar{C}_l = 2.4728$

Optimal actuated flow : $\bar{C}_l = 2.8207$



After 10 cycles of optimisation

- 14% improvement in mean lift over the initial actuated flow
- 29% improvement in mean lift over the un-actuated flow

2D SCCH High-Lift Configuration

Turbulent flow, $Re=10^6$, $\alpha=6^\circ$

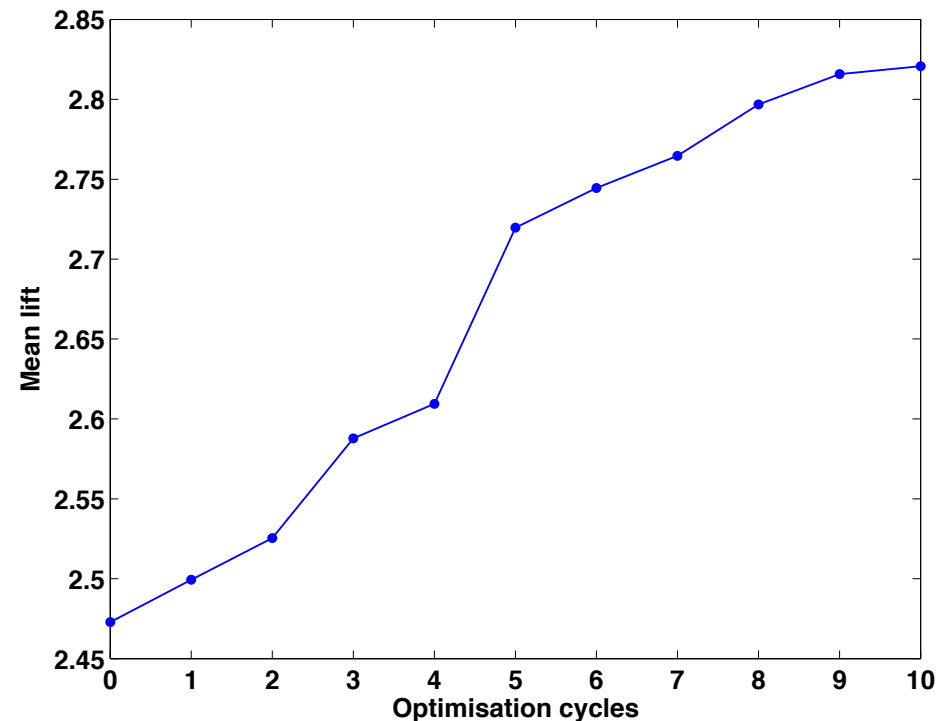
Optimal active flow control:

Optimiser: BFGS Quasi Newton Algorithm

Un-actuated flow : $\bar{C}_l = 2.1802$

Initial actuated flow : $\bar{C}_l = 2.4728$

Optimal actuated flow : $\bar{C}_l = 2.8207$



Optimization history: mean lift

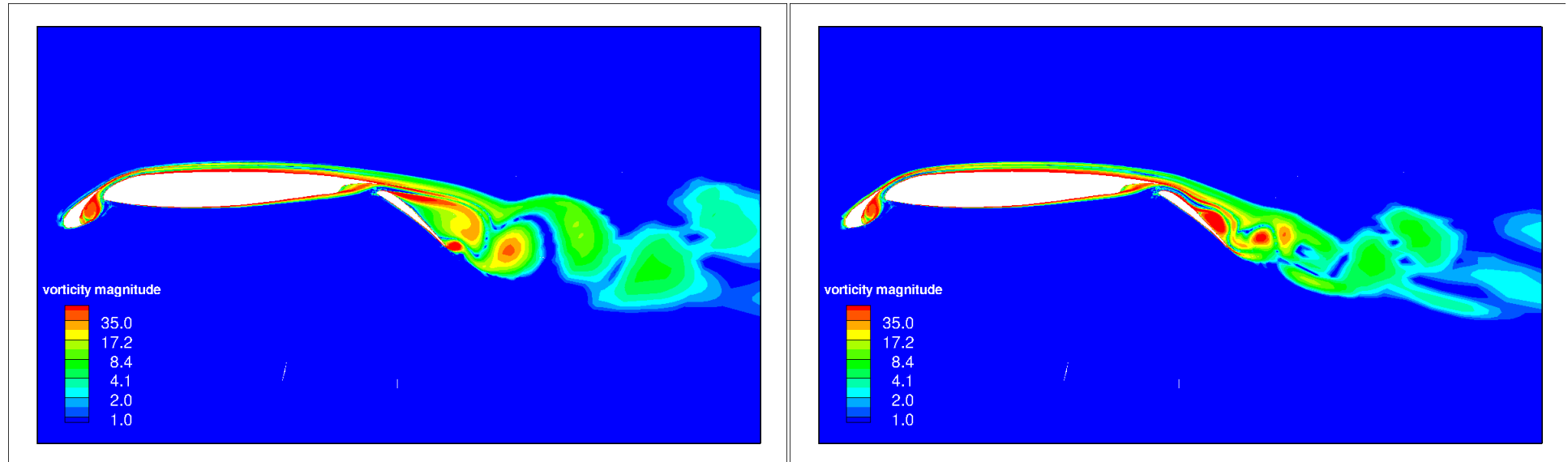
After 10 cycles of optimisation

- 14% improvement in mean lift over the initial actuated flow
- 29% improvement in mean lift over the un-actuated flow

2D SCCH High-Lift Configuration

Turbulent flow, $Re=10^6$, $\alpha=6^\circ$

Optimal active flow control:



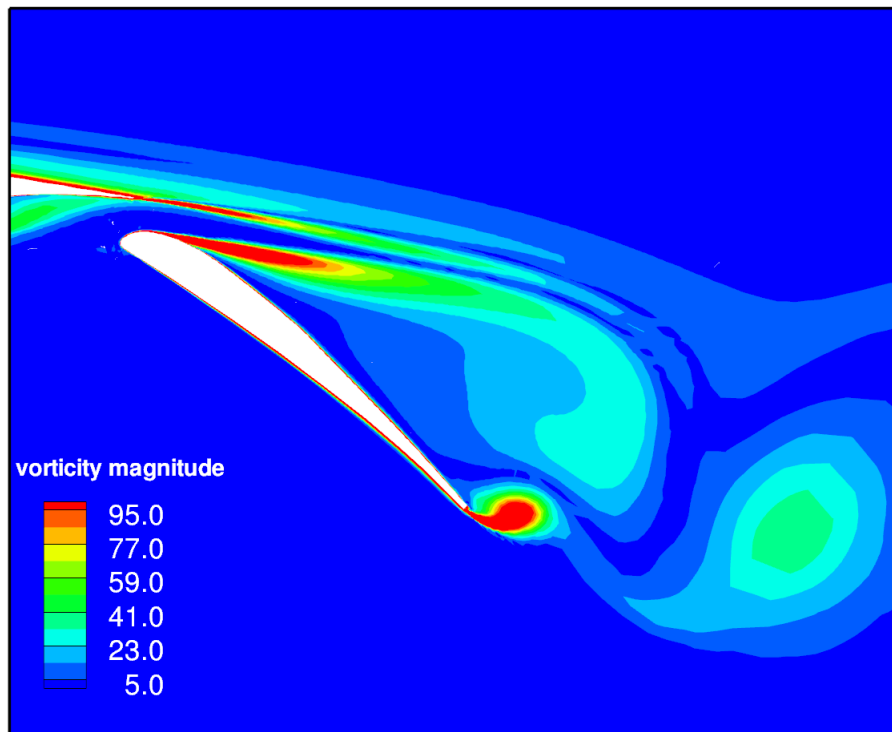
Un-actuated flow

Optimal actuated flow

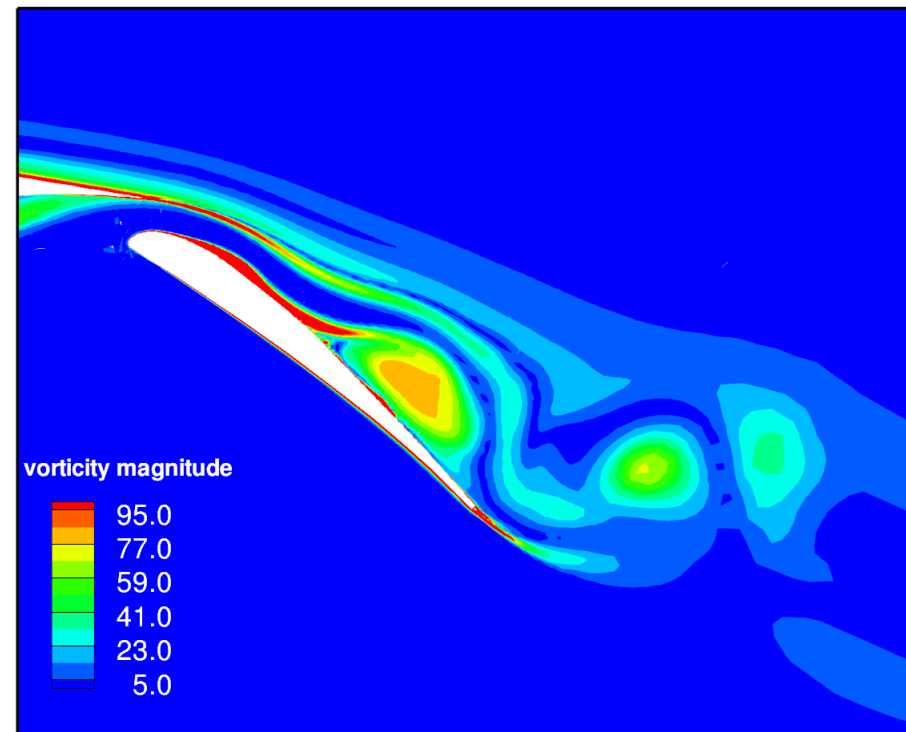
2D SCCH High-Lift Configuration

Turbulent flow, $Re=10^6$, $\alpha=6^\circ$

Optimal active flow control:



Un-actuated flow

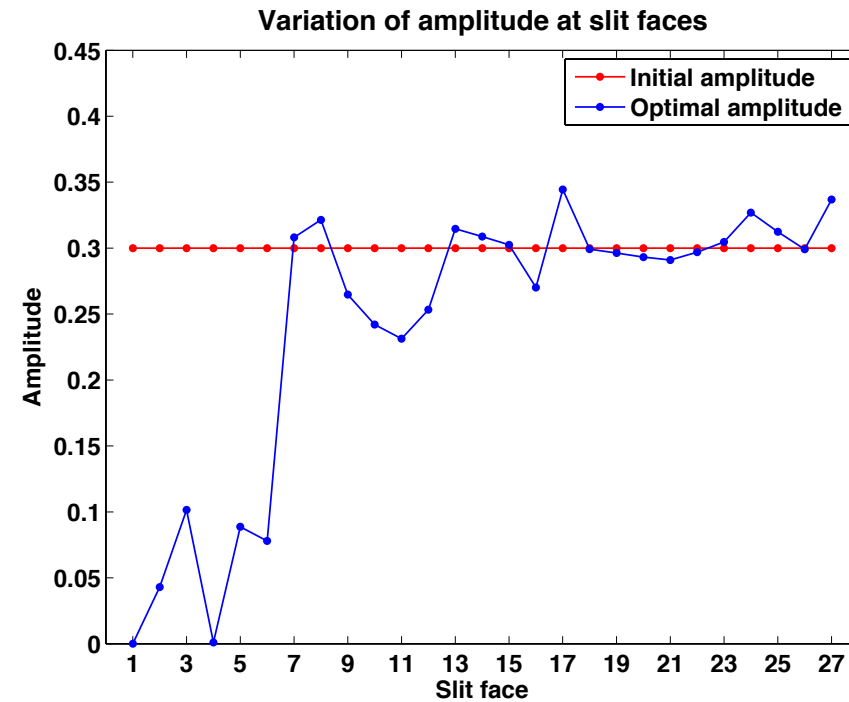
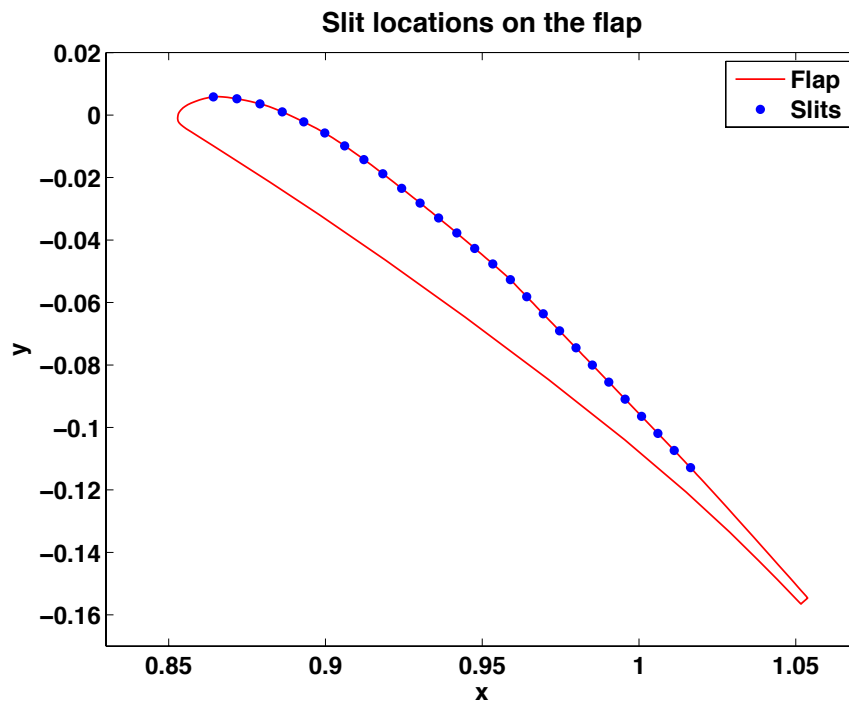


Optimal actuated flow

2D SCCH High-Lift Configuration

Turbulent flow, $Re=10^6$, $\alpha=6^\circ$

Optimal active flow control:

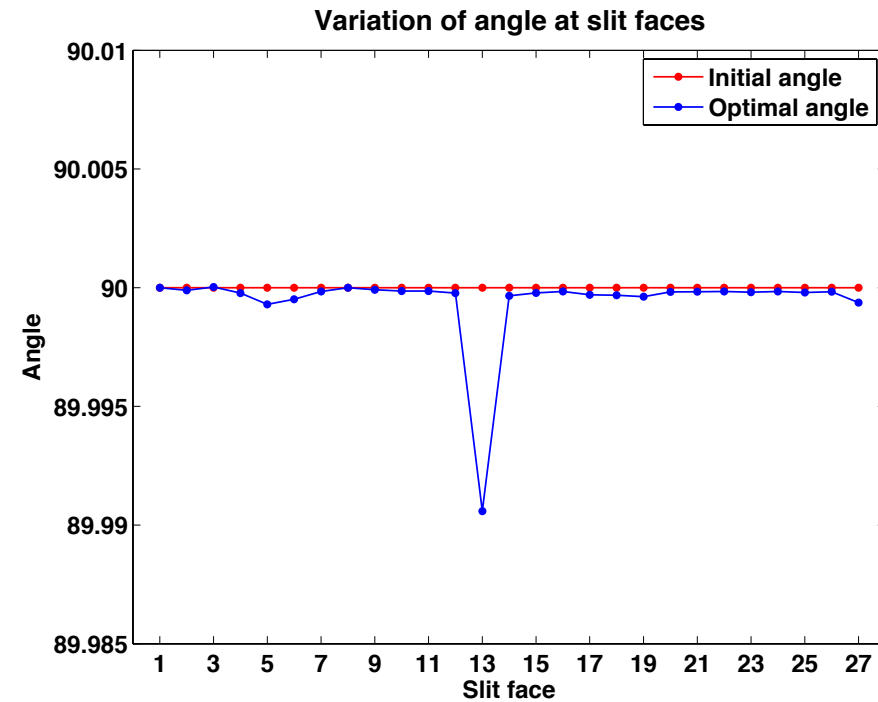
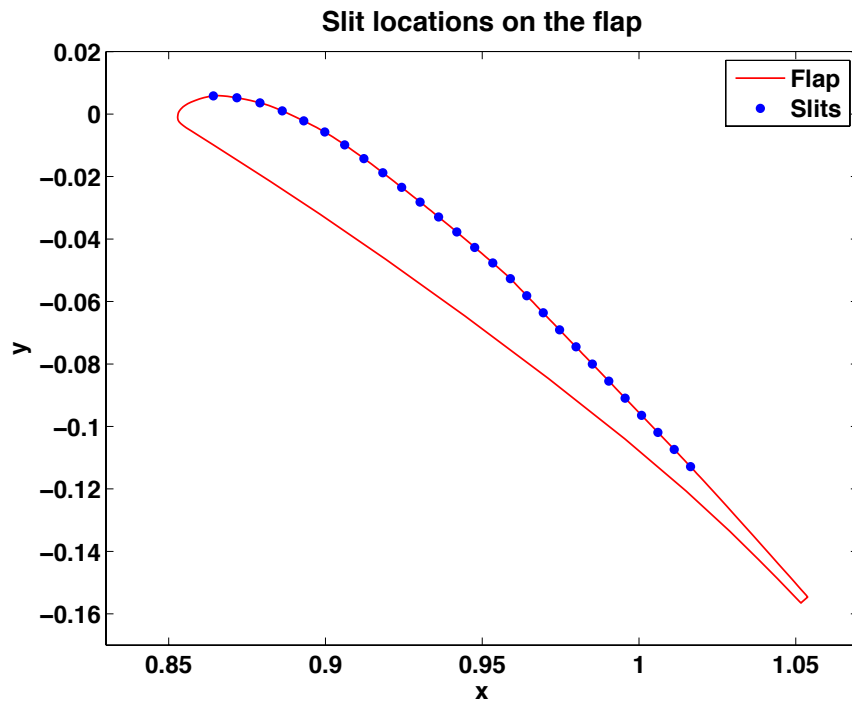


Initial and optimal distribution of amplitude at actuation slits

2D SCCH High-Lift Configuration

Turbulent flow, $Re=10^6$, $\alpha=6^\circ$

Optimal active flow control:

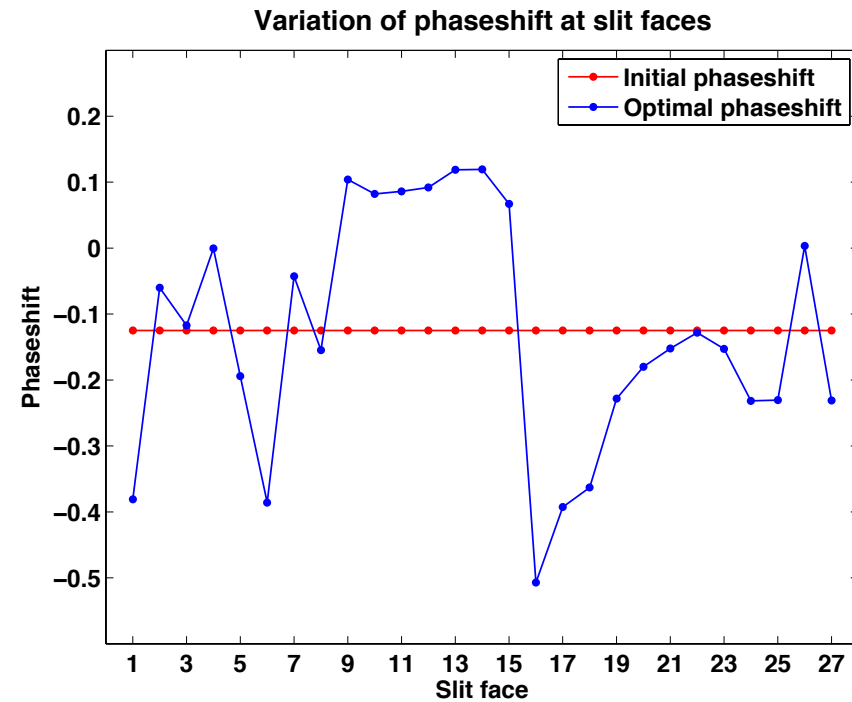
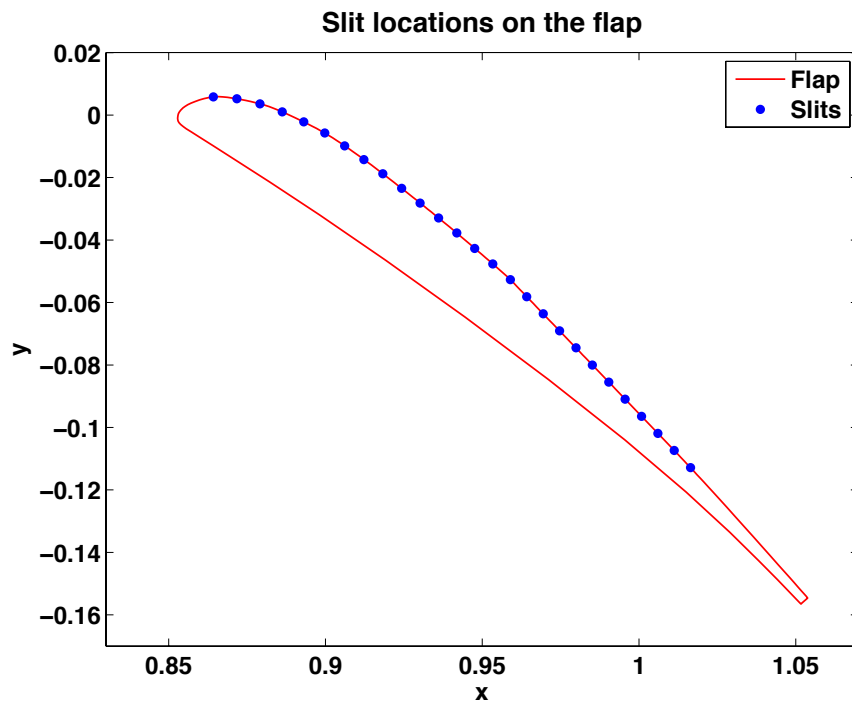


Initial and optimal distribution of angle at actuation slits

2D SCCH High-Lift Configuration

Turbulent flow, $Re=10^6$, $\alpha=6^\circ$

Optimal active flow control:



Initial and optimal distribution of phaseshift at actuation slits

Summary

Adjoint Approaches for Optimal Active Flow Control

- **Adjoint-based sensitivity evaluation (discrete, continuous, hybrid)**
- **Automatic/Algorithmic Differentiation (AD)**
- **Comparison continuous vs. discrete adjoint for cylinder case**
- **Checkpointing for unsteady adjoint computation**
- **Sensitivity study for 3D high-lift (SCCH) test case**
- **Optimal active separation control for 2D high-lift (SCCH) test case**

Outlook

- **Application of the consistent discrete adjoint approach to optimal active flow control for 3D high-lift (SCCH) test case, and ...**
- **... for the HIREX case!**

Thanks for your attention!